Energy, Entropy and Sustainable Development with Focus on Nuclear Fusion

Master Thesis in Theoretical Physics and Energy Physics

by

Susanne Flø Spinnangr

May 31, 2017

UNIVERSITY OF BERGEN

Department of Physics and Technology
University of Bergen
Norway

Contents

CHAPTER 1

Acknowledgements

I want to thank my supervisor Laszlo P. Csernai for his advice and guidance in my work on this thesis. I would never have imagined I would be able to participate on a published article before I had even finished my masters degree, and I am very grateful to Csernai for giving me this opportunity. I also want to thank my colleagues Sindre Velle and Yi-Long Xie for enlightening discussions and helping me figure out how to install and write in Latex.

My supporting family and friends also deserve a thank you for moral support and for being patient with me in my most stressed out moments, and I especially want to thank my friend Craig Grocott for proofreading.

CHAPTER 2

Abstract

The results of this thesis are twofold. First, based on the fundamental work of Ervin Schrödinger on sustainable development and its relation to entropy, we develop a program for discussing both the kinetic and configurational entropy of a system on the same level. This was published in Physica A in January 2017. The full article is included in the end of this thesis. The concept of entropy and sustainable development on Earth is connected in this first part. Second, the sustainability of different forms of energy production is discussed from a physical point of view, based on the concept proposed in the first part. Fusion energy is then highlighted based on conclusions made in the first and second part of the thesis. The discussion about sustainable energy production is at last put in context with the actual situation of energy production in Norway today.

CHAPTER 3

Introduction

One of the greatest challenges of our time is to solve the problem of sustainable development on Earth. It has long been known that the standard of living is directly connected to the availability of energy, and in order to ensure global sustainable development it is therefore fundamental to ensure sustainable energy development.

In this thesis, we try to illuminate an aspect of sustainable development that is often overlooked when discussing energy production. This is the concept of entropy production connected to the generation of energy, with special emphasis on electricity generation. In the fourth chapter, we will develop a method for discussing the thermodynamic entropy and information entropy on the same level for a given amount of material. We will illustrate how this affects physical systems by looking at the example of 1 kg water in different phases. This work, in addition to calculations done on more complex systems were published in Physica A in 2017, and the full article can be found at the end of this thesis.

In the fifth chapter, we systematically go through many of the important energy sources utilized today, discussing their sustainability based on their efficiency and entropy contribution to the Earth system.

In the sixth chapter, nuclear fusion energy is more closely examined, where we discuss some of the theoretical and technical aspects of a fusion power plant. Since thermonuclear fusion reactors with a large net energy output are still far away from being a reality, we will emphasize some of the obstacles that need to be overcome. Our group has for a long time been working on relativistic fluid dynamics in connection with the ignition of the fusion fuel in Inertial Confinement Fusion, and we will therefore focus more on this than on Magnetic Confinement Fusion.

Lastly, in the seventh chapter, we summarize the calculations regarding the sustainability

of the different energy sources and compare them to the current energy production in Norway.

CHAPTER 4

Entropy and Sustainability

4.1 The concept of entropy

When studying a system and its different states from a point of view of statistical mechanics, the concept of multiplicity is important. We say that the system is in a given macrostate, that can be measured or observed, and that a certain amount of microstates of the system can give rise to this particular macrostate. The number of possible microstates that can result in the given macrostate is the multiplicity of this macrostate. The second law of thermodynamics tells us that any large system in equilibrium will be found in the macrostate of the greatest multiplicity. Entropy is the measure of order in a system, and it is directly related to the multiplicity through the simple formula

$$S \equiv k_B \ln \Omega \tag{4.1}$$

where S is the entropy, k_B is the Boltzmann constant and Ω is the multiplicity. Since the logarithm is without a unit, the entropy adopts the unit of the Boltzmann constant, which is J/K in SI units. In the case of two interacting systems, A and B, the total entropy of the composite system can be known if we know the multiplicities of the systems A and B separately [12]. This is easily seen by the following relation:

$$S_{total} = k_B \ln \Omega_{total} = k_B \ln(\Omega_A \Omega_B) = k_B(\ln \Omega_A + \ln \Omega_B) = S_A + S_B \tag{4.2}$$

Even though the formula for entropy is simple enough, calculating a system's entropy is not always straight forward. When a system starts to become large, it is impossible to simply count the number of possible microstates, and we must therefore estimate the multiplicity in other ways, using statistical methods. This implies simplifications and assumptions about the system that will vary in accuracy depending on the state of the

system. As an example, the formula for the entropy of a monatomic ideal gas is

$$S = Nk_B \left[\ln \left(\frac{V}{N} \left(\frac{4\pi mU}{3Nh^2} \right)^{\frac{3}{2}} \right) + \frac{5}{2} \right] \tag{4.3}$$

where N is the particle number, V is the volume, U is the internal energy, m is the atomic mass and h is Planck's constant. This equation is known as the Sackur-Tetrode equation [12], and a modified version of this formula is used in a later section where we calculate the entropy of different phases of water.

From statistical physics and quantum mechanics we know that in a closed system there will always be a tendency towards an eventual stabilization at the most probable macrostate. This is the state of thermodynamical equilibrium, which is also the state with the highest entropy. This theory is the basis for the hypothesis that eventually the entire universe will end up in a state of maximum entropy. This is what is called 'The Heat Death of the Universe'. This has also been proposed to happen with the Earth [2]. By closer examination it is clear that this is not true for the Earth since it receives energy from the Sun and can therefore not be considered a closed system. This interaction will be discussed further section 4.4 in the context of life on Earth and sustainable development.

The discussion of entropy so far in this chapter has only been concerned with the thermodynamical definition of entropy. It is based on the interaction of particles with a certain temperature and different degrees of freedom such as translation, rotation and vibration. This is not the only basis of entropy. Also of importance is the Shannon entropy of a system. It is a form of information entropy that is associated with the configuration and complexity of the system. We can calculate the Shannon entropy of a system if we know the number of possible discrete states, n, the system can be in, and the probability of each state p_j with $j = 1, 2, ..., n$. The entropy of that system, H_i, is then defined as the sum

$$H_i = -\sum_{j=1}^{n} p_j \ln p_j \tag{4.4}$$

where $\sum_{j=1}^{n} p_j = 1$ [16] (in his original equation, Shannon also included a positive constant K in front of the sum, but this only affects the choice of measuring unit). This equation goes to an integral when the states of the system are not discrete, and the probabilities p_j goes to a probability density function, $p(x)$

$$H_i = -\int p(x) \ln p(x) dx \tag{4.5}$$

with the normalization $\int p(x)dx = 1$ and where the integrals are evaluated over the range of x. The limits on the integrals will therefore depend on the system [14]. If the system undergoes a process that leads to a change in the values of p_j or the shape of $p(x)$ the system will have a new entropy, H_f. The change in entropy between the two states of the system can then be expressed as $\Delta H = H_f - H_i$ or $\Delta H = H_f(x) - H_i(x)$ for a continuous distribution of states [14]. In his article [16], Shannon interpreted this entropy as a measure of the uncertainty about the state of the system, and an increase in information about the system therefore represents a decrease in the system's entropy. If we let ΔI represent the change in information known about the system we can then

write $\Delta I = -\Delta H$ [14]. A more complex system will therefore have a lower entropy, since it contains more information than a system of lower complexity. The above definition of entropy was introduced by Claude Shannon in 1948 in the context of information theory [16]. However, as Shannon pointed out, this H is the same as that which Boltzmann already used when he developed his H-theorem for non-equilibrium systems if we let the p_i be the probability that the system is in cell i of its phase space [1] [15] [16]. As will be described in section 4.2, this makes us able to attribute the same physical dimensions to both Shannon entropy and thermodynamical entropy. The idea of an increased amount of information being the same as a decrease in the amount of entropy in a system was also discussed by Brillouin [17]. He used the term *negentropy* to describe a negative entropy change in a system, which corresponds to an increased amount of information. He also attributed negentropy to be a measure of a closed system's possibility for doing mechanical or electrical work. As discussed later in chapter 5, this is consistent with the calculations of the Carnot efficiency of a heat engine, where the work done is related to the different values of entropy in the engine during a cycle.

4.2 A quantitative method for calculating entropy

As mentioned in section 4.1, different definitions of entropy exist in, for example, physics and information theory, and all are equally valid. It is therefore of interest when discussing the entropy of a system to be able to include different types of entropy on the same level. A method for doing this that is applicable for both simple and complex systems is developed in this section. This makes us able to calculate the entropy of a well-defined amount of matter irrespective of what type of matter is discussed. Since this entropy is uniform for all matter, it makes us able to compare the entropy of different types of matter. This had not been done before when we developed it, and the method with calculations and estimations have been published in Physica A [1]. The full article is attached at the end of this thesis, but only the development of the method and calculations for the entropy of 1 kg of water during phase changes will be included in this thesis.

In this section, we first introduce a method for calculating the thermodynamical entropy, and the entropy of 1 kg of water is calculated using this method. Next, a way of calculating the configurational entropy is introduced and again implemented on 1 kg water. The section is concluded by showing how these two entropies can be combined.

In order to be able to calculate the entropy of a system, some assumptions about the state of the system must be made. The real entropy value will therefore differ from the calculated value to different degrees depending on the validity of the assumptions. In our example, we want to calculate the entropy of 1 kg of water in all its three phases. If we start with steam at 100^oC and atmospheric pressure, we can assume that the steam can be approximated as an ideal gas. We can then use a modified version of equation (4.3) to calculate its entropy. For 1 kg water vapor, we can express equation (4.3) in terms of the particle number N_p, particle mass m_p, particle density n_p, and gas temperature T [1]

$$S_{1kg} = N_p\, k_B \left[\ln\left(\frac{(2\pi m_p c^2 kT)^{\frac{3}{2}}}{n_p (2\pi\hbar c)^3} \right) + \frac{5}{2} \right] \tag{4.6}$$

The particle density can be found in terms of Avogrado's number, $A_v = 6.022{\times}10^{23}\, mol^{-1}$, and the molar volume of an ideal gas, $V_{IG} = 0.0224\, m^3$ at standard temperature and pressure (STP where T = 273.15 K, P = 1 atm). These values give us a particle density of $n_p = \frac{A_v}{V_{IG}} = 2.688 \times 10^{25}\, mol^{-1} m^3$. The particle mass can be found in the unit of kg by multiplying the nucleon mass, m_n, with the mass number of the particle, A_p. For water, $A_p = 18$ (H + H + O = 1 + 1 + 16 = 18) and $m_n = 1.661 \times 10^{-27}\, kg$, giving us $m_p = A_p \times m_n = 2.989 \times 10^{-26}\, kg$. Using equation (4.6) with the values for water ($A_p = 18\, u$, $N_p = 55.116\, mol/kg$, $1kg = 55.56\, mol$) at STP gives us an entropy of $S_{1kg} = 7993.0\, J/K$. Letting the temperature be the actual boiling temperature of water ($T = 373.15\, K$) we get an entropy of $S_{1kg} = 8243.0\, J/K$. Here we need to keep in mind that since the molar volume is temperature dependent, so is the particle density, and using equation (4.6) with $T = 373.15\, K$ will give a slightly wrong estimate if we do not also find the molar volume of water vapor at $T = 373.15\, K$. However, since we here are interested in showing how the entropy changes with temperature (and later with complexity) rather than finding exact values, we still use this value for different temperatures.

When we later want to combine the thermodynamic entropy and the configurational entropy, we need to make these values unitless. This is done by dividing the S_{1kg} value on the Boltzmann constant and the particle number, giving us a unitless specific entropy per particle

$$\sigma_p = \frac{S_{1kg}}{k_B N_p} \tag{4.7}$$

The specific entropy of 1 kg water at STP and at 100^oC and $P = 1$ atm is then $\sigma_p = 17.442$ and $\sigma_p = 17.988$ respectively. As we can see from this equation, the term in brackets in equation (4.6) gives the entropy for one particle.

The values for the entropy of water vapor calculated in the ideal gas approximation will underestimate the value since it does not take into consideration the interaction between the water molecules and the internal vibrational degrees of freedom. However, it is of interest since it can be considered an estimated minimum value of the entropy of the gas. When the temperature is decreased, water will go through phase changes to liquid water and solid ice. With each phase change when the temperature is decreasing, the degrees of freedom are reduced and consequentially the value of the entropy decreases. As the temperature and thermodynamical entropy decrease, the importance of the configurational entropy increases since much more of the information about the system is contained in the interaction and configuration of the molecules in the system.

In order to calculate the entropy in the liquid phase of water, we need measurable values that can be related to the entropy change. As the phase changes are driven by the internal energy of the water, we want to try to connect the entropy and the internal energy of a system. Temperature is defined through the concept of heat flow. From experiments and everyday experience, it is known that heat spontaneously flows from a system of higher temperature to a system of lower temperature if they are not closed. When the

two systems reach thermal equilibrium, they will have the same temperature, and the heat flow will stop. At this thermal equilibrium, the total entropy of the interacting system will have reached its maximum value. We can express this mathematically by considering how the entropy changes versus the internal energy in the systems. If we call the two systems A and B, we can express the slope of the entropy change at equilibrium as [12]

$$\frac{\partial S_{total}}{\partial U_A} = 0 \tag{4.8}$$

We know from equation (4.2) that $S_{total} = S_A + S_B$, allowing us to write

$$\frac{\partial S_A}{\partial U_A} + \frac{\partial S_B}{\partial U_A} = 0 \ , \tag{4.9}$$

at equilibrium. By keeping the total energy of the two interacting systems constant, we can interchange ∂U_A with $-\partial U_B$, allowing us to write

$$\frac{\partial S_A}{\partial U_A} = \frac{\partial S_B}{\partial U_B} \tag{4.10}$$

at equilibrium. From this, we can define the temperature of a system as the slope of the entropy versus energy change in the system [12]

$$T \equiv \left(\frac{\partial S}{\partial U}\right)^{-1} \ . \tag{4.11}$$

Since measuring entropies is very difficult, we can rather use this definition to calculate it through measuring more accessible variables. The heat capacity of a system at constant volume and particle number is defined as

$$C_V \equiv \left(\frac{\partial U}{\partial T}\right)_{N,V} \ . \tag{4.12}$$

Combining the definition of temperature (equation (4.11)) and this definition of the heat capacity, we can say that if the volume and particle number are held constant while heat is provided to a system, and no other work is done to it, its entropy will change by the amount

$$dS = \frac{C_V dT}{T} \ . \tag{4.13}$$

This equation can be used to calculate how the entropy behaves when the temperature of the water is changed. It is valid for all phases of water provided that the heat capacities are correct. By choosing a reference value for the entropy, we can integrate dS for given temperature steps. In our paper [1] we chose the reference point to be at $T = 100^oC$ liquid water which has the entropy $S_{1kg} = 4430.01\frac{J}{K}$. We calculated the values for ΔS in steps of $\Delta T = 10K$, giving us the equation

$$\Delta S = \Delta T \left(\frac{C_{V1}}{T_1} + \frac{C_{V2}}{T_2}\right) \ . \tag{4.14}$$

This gives the entropy difference between the temperatures T_1 and T_2. Since we know the entropy decreases with the temperature, we can calculate the entropy of the water at T_2 when we know the value at the higher T_1 by subtraction

$$S_2 = S_1 - \Delta S \ . \tag{4.15}$$

During a phase change, the temperature of the system remains unchanged while the internal energy either increases or decreases. From the 2nd law of thermodynamics, we can define entropy change through heat flow and temperature

$$dS = \frac{dQ}{T} \tag{4.16}$$

where dS is entropy change, dQ is heat entering or leaving the system, and T is the temperature of the system. If we use the latent heat of the phase change as dQ and keep the temperature constant, we can use this to calculate the entropy change of a phase change. For 1 kg water, the latent heat of vaporization is $dQ_v = 2257 \times 10^3 J/kg$, while the latent heat of fusion is $dQ_f = 3.35 \times 10^5 J/kg$ [1]. The results of these calculations are plotted in figure 4.1 (for the S value with $T > 100^oC$ we simply exchanged the - with a + in equation (4.15)).

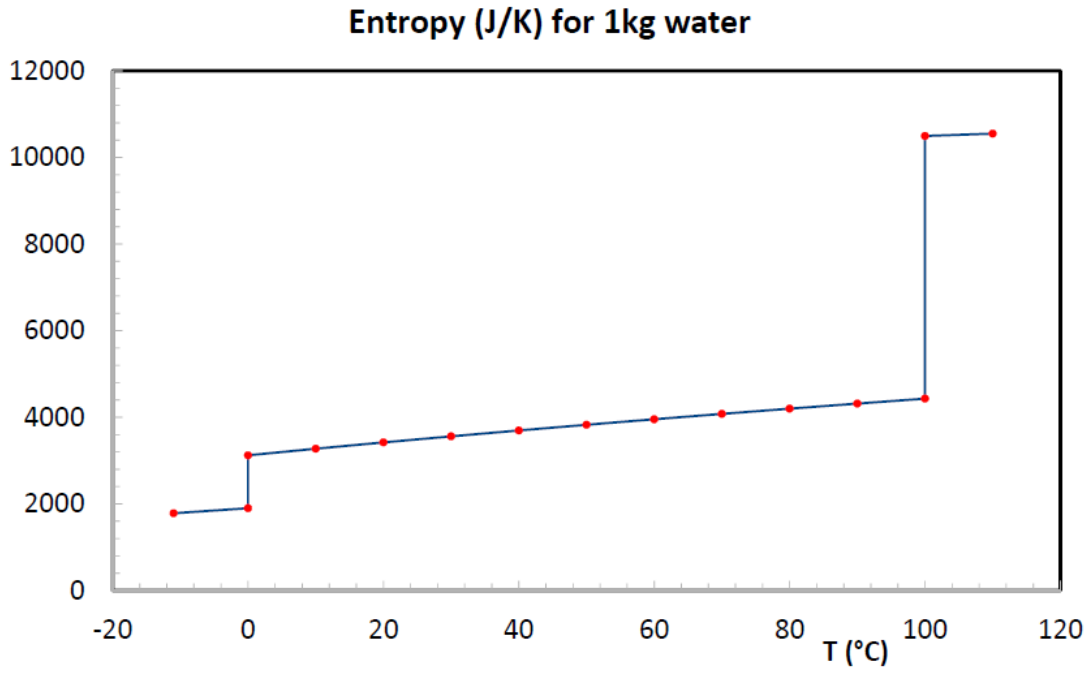

Figure 4.1: The entropy of 1 kg water as a function of temperature. Values to note are the reference point at $T = 100^oC$ liquid water with $S_{1kg} = 4430.01 J/K$, the entropy of water vapor at $T = 100^oC$ with $S_{1kg} = 10495.56 J/K$, the entropy of liquid water at $T = 0^oC$ of $S_{1kg} = 3122.92 J/K$ and that of ice at $T = 0^oC$ with $S_{1kg} = 1900.15 J/K$. The entropy change of the phase transitions has been calculated using the latent heat. From [1]

The above discussion gives us a way of estimating the kinetic entropy of a system. We now need a method for estimating the configurational entropy of a system, and a way to combine these. The configurational entropy can be calculated using topological arguments by first imagining a set of hypothetical ideal gases constructed of nucleons from H_1, H_2, H_3 and H_4. We neglect all other contributors to the entropy than the topologies of the binding or link between them. For H_1 there is no link since there is only one nucleon, and for H_2 there is only one link between two nucleons. However, this link can only be inserted one way, and its topology therefore does not contribute any additional entropy. In other words, the values of p_i and i in equation (4.4) are both = 1, and we have

$$H(X) = -p_1 \ln p_1 = 0 \tag{4.17}$$

When $N > 1$ the entropy will be given by equation (4.4) and have a maximum at the most random configuration, which is when $p_i = \frac{1}{N}$ for each i so that

$$H(X) = -\sum_{i=1}^{N} p_i \ln p_i = -N \frac{1}{N} \ln \frac{1}{N} = H_{max} \tag{4.18}$$

If we further consider the case of H_3, the nucleons can be combined by either 2 or 3 links, giving us two characteristic structures for 3 nucleons. If we label the nucleons 1, 2 and 3, the links between them can in the case of two bindings be inserted three ways, either between 1&2 and 2&3, or 1&3 and 2&3, or 1&3 and 1&2. In the case of three links, there is only the one way they can be inserted, 123. If we imagine that we start with the three link configuration, the different configurations with two links can be obtained by cutting one link, which can be done in three different ways, see figure 4.2.

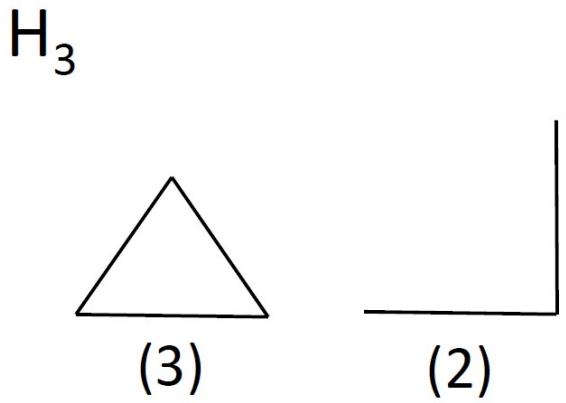

Figure 4.2: The possible topological configurations of a H_3 molecule

Letting $i = 1$ be the three links configuration and $i = 2$ be the two links configurations, we obtain the values $p_1 = 1/4$ and $p_2 = 3/4$ for their probabilities. Inserting this into equation (4.4) we obtain for the entropy

$$H(X) = -[\frac{1}{4} \ln \frac{1}{4} + \frac{3}{4} \ln \frac{3}{4}] = 0.5623 \tag{4.19}$$

We can continue the same reasoning for the case of H_4, where we can have between 3 and 6 links. Since water is a H_3 molecule, the further explanation of this hypothetical gas is omitted here, but interested readers are referred to chapter 3 in [1]. The Shannon entropy values for the H_4 case if all the possible configurations are realized is $H(X) = 1.5526$. We see from this that the entropy is already three times as large. In physics, not all hypothetical configurations are realized, and the links are not necessarily indistinguishable since they can have different energies, meaning that the estimated probabilities will vary from the real, measured probabilities. However, this discussion still shows that the topological entropy should be taken into account when we want to calculate the total entropy of a system. In order to do that, all contributions to the entropy need to be in dimensionless form. The Shannon entropy already is dimensionless, and as shown earlier in this section, the thermodynamical entropy as given by equation (4.6) can easily be made to be dimensionless. Boltzmann defined the entropy for any non-equilibrium system in the same form as the Shannon entropy, and we can therefore write for one particle

$$H(X) = \sigma_p = \frac{S}{k_B N_p} = -\sum_{i=1}^{N} p_i \ln p_i \tag{4.20}$$

This may define both the sum of all the configuration probabilities, p_i^c, or the sum of all probabilities for the particle to be in a phase space volume element of size $(2\pi\hbar)^3$, p_i^p. These probabilities can be calculated using the phase space distribution function, $f(x,p)$ normalized for one particle,

$$p_i^p = (2\pi\hbar)^3 f(x,p) \tag{4.21}$$

For a relativistic gas, we can find the entropy density in a system, $s(x)$, using Boltzmann's definition of the phase space distribution for any equilibrium or non-equilibrium system [18]

$$s(x) = -\int \frac{d^3p}{p^0} p^\mu u_\mu f(x,p)[\ln((2\pi\hbar)^3 f(x,p)) - 1] \tag{4.22}$$

where $p^\mu u_\mu$ is the frame invariant, relativistic expression for the local energy density. In the event of an equilibrium state, the Boltzmann Transport Equation reaches a stationary solution and the phase space distribution takes the form of a Jüttner distribution

$$f(x,p) = f^{Juttner}(p) = \frac{1}{(2\pi\hbar)^3} exp\left(\frac{\mu - p^\mu u_\mu}{T}\right) \tag{4.23}$$

where T is the temperature of the system and μ is the chemical potential (the μ indices on the momentum and velocity four-vectors are still just the contravariant and covariant summation indices of the four-vector product). The Jüttner distribution describes the particle momentum distribution in a thermal system which is moving with velocity u^μ and has the chemical potential μ and temperature T [18]. By inserting equation (4.23) into equation (4.22) and keeping in mind that for a stationary solution we have $p^\mu u_\mu = p^0$ we get the following expression for the entropy density

$$s(x) = -\int d^3p f(x,p)\left[\frac{\mu}{T} - \frac{\varepsilon}{T} - 1\right] \tag{4.24}$$

where $\varepsilon = p^\mu u_\mu = p^0$ is the specific energy for one particle. If we now normalize the phase space distribution such that

$$n_p(x) = \int d^3p f(x,p) \tag{4.25}$$

then the thermodynamic specific entropy for one particle can be obtained as in equation (4.20), and we get for the entropy of the phase space

$$\sigma_p^{ph.s.} = \frac{s}{k_B n_p} = -\sum_{i\,\epsilon\,ph.s.} p_i^p \left[\ln p_i^p - 1\right] \tag{4.26}$$

The p_i^p terms are the occupation probabilities of the i phase space cells, and should be calculated for one particle such that $\int d^3x\, n_p(x) = 1$. We can now conclude that in the single particle case, the entropies of the configuration space and the phase space should be additive and we get the following dimensionless expression for the total entropy

$$\sigma_p = \sigma_p^{conf.} + \sigma_p^{ph.s.} = -\sum_{i\,\epsilon\,conf.} p_i^c \ln p_i^c - \sum_{i\,\epsilon\,ph.s.} p_i^p \left[\ln p_i^p - 1\right] \tag{4.27}$$

where p_i^c is the probability of having the configuration state i. The possibility of having different topological configurations leads to an increase in the number of degrees of freedom for the single particle, which leads to an increase in the entropy of this particle. In table 4.1 the calculated entropy values for the H_1, H_2 and H_3 hypothetical ideal gases are calculated using equation (4.27). We see that for the H_3 the specific entropies increase with the relatively small amounts of 0.347 and 0.216 for the two different topological configurations $H_3^{(3)}$ and $H_3^{(2)}$.

Material	A_P	N_P (mol)	σ_P	S_{1kg} (J/K)
H_1	1	992.092	13.106	108111.7
H_2	2	496.046	14.146	58344.0
H_3	3	330.697	14.754	40568.3
$H_3^{(3)}$	3	330.697	15.101	41521.2
$H_3^{(2)}$	3	330.697	14.970	41161.6

Table 4.1: Entropies of a single composite particle and of 1 kg material in different topological configurations for the hypothetical H_1, H_2 and H_3 molecules approximated as ideal gases, depending on the mass numbers, A_p, of the nucleons in the molecule and the configuration where it is indicated. Recreated from table 2 in [1].

In the case of water, we can consider it as a H_3 molecule since it consists of two hydrogen atoms and one oxygen atom. However, there is a major difference to consider. Since all the particles are not identical in a water molecule, the configuration with two links have three possible topologies, see figure 4.3.

In addition, in real physical molecules, the entropy might be lower than that which is calculated here since more complexity can be contained in the molecule due to, for example, direction dependence of the links, different constituents, different (energetic) weights

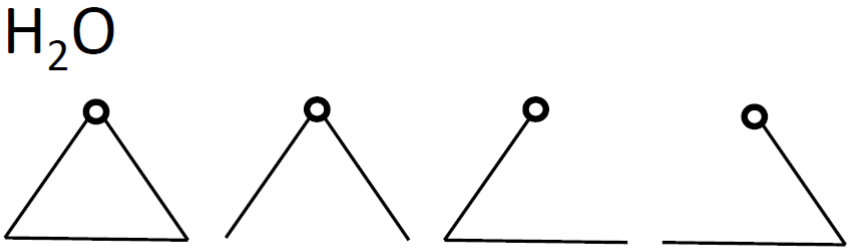

Figure 4.3: The four hypothetically possible topological configurations of a water molecule. The circle marks the position of the oxygen atom. Only the second configuration is realized in nature, and if the two hydrogen atoms are identical at least two of the configurations are also identical. From [1].

of the links, dynamical freedom of the length or angle of the links etc. If we estimate the thermodynamical entropy of water vapor at 100^oC using the ideal gas approximation (equation (4.6)) we get a the value $S_{1kg} = 8243J/K$, which is lower than the measured value of $S_{1kg} = 10495.56J/K$. This can be due to the different constituent atoms, H and O, the configuration and other dynamical degrees of freedom and types of interactions. We can use equation (4.20) to calculate the Shannon entropy of the different topological configurations shown in figure 4.3 and see how this affects the total entropy value. The two hydrogen atoms can either be considered distinguishable or indistinguishable, which will give rise to two different expressions for the configurational entropy. Also, we can either have all the configurations realized ($N = 4$ or $N = 3$ depending on whether or not the hydrogen atoms are unique), or only a single configuration. Assuming first that all the topological configurations have equal probabilities, the specific topological configuration entropies can be calculated as

$$\sigma_p^{conf.} = -\sum_{i=1}^{N} p_i \ln p_i = \ln N \qquad \text{or} \qquad \sigma_p^{conf.} = -p_i \ln p_i \tag{4.28}$$

for all configurations or a single one respectively. The results of these calculations are summarized in table 4.2, where the phase space entropy, $\sigma_p^{ph.s.} = 17.988$ for 100^oC water vapor as an ideal gas is calculated using equation (4.7) and added to the configurational entropies.

We see that, if more than one of the configurations is realized, it leads to a higher entropy value than if only one configuration is realized. Knowing that only one configuration is realized is a gain in the amount of information we have of the system. The lower entropy value in this case is in accordance with the discussion earlier in this chapter about how a gain in information is the same as a reduction in the entropy value. We know that for a real water molecule, only the second configuration in figure 4.3 is realized, and the hydrogen atoms are identical. Therefore, the realistic entropy values for a water molecule are calculated using $N = 3$ and the second expression in equation (4.28), and the results of this are highlighted in table 4.2. As we see for the corresponding values

	All 4	All 3	One of 4	One of 3
$\sigma_P^{conf.}$	1.386	1.099	0.347	**0.366**
σ_P	19.374	19.087	18.335	**18.354**
$S_{1kg}^{conf.}$ (J/K)	635.1	503.63	159.02	**167.7**
S_{1kg} (J/K)	8878.3	8746.8	8402.2	**8410.9**

Table 4.2: Topological configuration entropy and total entropy of 100^{o}C water vapor. The realistic physical case is in the last column. From [1].

for 1 kg material, adding the configurational entropy to the ideal gas approximate moved the calculated value ($S_{1kg} = 8243.0J/K$) closer to the experimentally observed value ($S_{1kg} = 10495.56J/K$). If we had taken into account other degrees of freedom, such as the angle between the hydrogen atoms and the variability of the distance between the atoms, the energetic configuration of the water molecule in the vapor, or not approximating it as an ideal gas, we would have come even closer to the experimental value.

We have chosen to do these calculations for water vapor since this allows us to compare the values from the ideal gas approximation with the relatively well-known experimental values for vapor. In order to be able to carry out comparisons of the entropy content, a common reference point must be used. Since we know from the theorem of Nernst that the entropy must be exactly 0 when the temperature is 0 K, it could be argued that this would be a good reference point. However, the experimental values for ice are less known since several different configurations for ice exist, and it is very difficult to measure the entropy values near 0 K. Since we do not know much about how the entropy would behave in the large temperature range between 0 K and 0^oC, this could potentially affect the entropy values greatly, and make our estimates wrong. For simple structures such as water, we have experimental values we can compare with our calculations. This is not true for more complex structures, such as organic materials. In [1], we make estimates using the method outlined in this section for estimating the entropy content of complex molecules such as the bacterial DNA molecule, the CCr bacterium and the human genome, but these discussions will not be included in this thesis. We have already seen in the water example that the ratio between the kinetic and configurational entropy changes dramatically with the internal energy of the system. As we see in figure 4.1, the kinetic entropy value significantly decreases between vapor and liquid water at 100^oC, while the configurational entropy should be relatively constant. This leads us to assume that the configurational entropy contribution will be more important in comparison with the kinetic contribution as the complexity of the system increases [1].

4.3 Entropy and life

As we saw in the previous section, entropy estimates for different structures can be done for a finite amount of material. In 1944, Erwin Schrödinger published his book *What is Life* [11]. In it, he discusses what features are characteristic of living systems in contrast to inanimate systems, and whether or not life can be explained by the known physical concepts. When energy is deposited into a system, basic physics tells us that it is possible to have a negative entropy change in the system. Schrödinger comes to define 'life' as some structure or system that spends energy actively to decrease its own entropy. This means that something that, through various processes, takes structures with higher entropy and builds more complex structures of lower entropy from them can be considered to be alive. He says:

> "Life seems to be orderly and lawful behavior of matter, not based exclusively on its tendency to go over from order to disorder, but based partly on existing order that is kept up. (...) The living organism seems to be a macroscopic system which in parts of its behavior approaches to that purely mechanical (as contrasted with thermodynamical) conduct to which all systems tend, as the temperature approaches the absolute zero and the molecular disorder is removed." [11].

At the time when Schrödinger wrote his book, the structure and properties of the DNA, or "the hereditary substance" as he called it, was not well known, and not enough was known about living structures to make any quantitative calculation on the entropy of living organisms. Today, we know enough about the structure of the DNA molecule as well as the other constituents of a living cell to be able to make quantitative estimates about the entropy of living organisms, as we did in [1]. Estimations of the entropy of different species have also been connected to the life expectancy of that species [19]. Schrödinger concluded that if life is defined as something that feeds on negative entropy, then a living organism will die when complex, low entropy food is not available, or when its entropy grows beyond a limit.

In [13], Chyba and McDonald discuss the definition of life in a terrestrial and extraterrestrial perspective. In their discussion about the origin of life on Earth, they highlight how there have been two distinct approaches when trying to answer this question based on two different definitions of life. In the Darwinian definition, life is defined to be "a system capable of evolution by natural selection" [13], which is also referred to as the genetic definition. This definition has later been refined by several scientists [13], most importantly in this context to include the word "self-sustaining", which was introduced by Joyce in 1994 [13]. The inclusion of 'self-sustaining' as a criterion mean that a living system must undergo some kind of metabolism. The reason for the two different definitions of life then stems from the question of the origin of life: was it the origin of genetic material or of metabolism? With the discovery of RNA, these two need not be separate anymore, and the Darwinian definition of life is one of the most accepted definitions today [13]. In the context of this discussion it is therefore important to consider whether or not the Darwinian definition of life is compatible with Schrödinger's definition from 1944. Chyba and McDonald [13] define metabolism with a basis in thermodynamics, the

same as Schrödinger:

> "Because of the Second Law of Thermodynamics, a living system can only remain alive if the production of entropy is offset by an input of energy or energy-rich matter. Metabolism is then no more than the turnover of free energy that makes it possible for a given system, compartmentalized or not, to avoid reverting to an equilibrium state of maximum entropy. In this sense, the chemical Darwinian definition of life includes both genetic and metabolic components."

It then seems that the Darwinian and Schrödinger's definitions are compatible, although the Darwinian definition is more restricting. The quest to give a clear definition of what life is has proven to be very difficult. We are only able to study terrestrial life, and even this comes in so many variations that virtually every definition we have today seems to either exclude organisms that are clearly alive or include systems that are generally not considered alive [13]. Even though the Darwinian definition of life is one of the most accepted definitions today, it can be argued that it excludes systems that are generally thought of as alive. By definition, it requires that life is a chemical system capable of metabolism and Darwinian evolution, which then excludes biological viruses since they need other living cells for the replication process of their DNA or RNA strands [32]. Schrödinger's definition of life can be categorized as a *thermodynamical* definition, and it would include biological viruses. However, it can be argued that it also includes crystals, which are not considered to be alive [32]. In the context of this thesis, we do not intend to make any claim about which definition of life is the correct one, if such a definition even exists. We only seek to highlight that most organisms that are considered to be alive are included in the definition provided by Schrödinger in 1944, and that the existence of life on Earth as Schrödinger defines it contributes to sustainable development. In the next section, we will make the connection between sustainable development and decreasing entropy.

4.4 Entropy and sustainable development

It is not difficult to understand that the Earth is a system with a limited availability of territory and material resources. Arguably, the most important and complex question of our time is how we are going to achieve sustainable development in such a system. The term 'sustainable development' as we use it today was defined in the UN commissioned report *Our Common Future* in 1987. It is stated there that sustainable development is development that "meets the needs of the present without compromising the ability of future generations to meet their own needs" [10]. With the increase in the global human population that we observe today, it is not necessarily easy to imagine how we can have any form of development and general increase in life standard without jeopardizing life for future generations. The standard of living is directly proportional to energy consumption. Increasing consumption in the already industrialized countries in the world, in addition to the rapidly industrializing countries such as China and India, leads to the projection of future energy consumption to be at least doubled by the year 2100 [9]. In order

to have sustainable societal development, it is therefore important to have sustainable development in energy production.

If we extend the previously mentioned Earth system to an Earth-Sun system, we can consider the exchange of energy between the Earth and the Sun with our environment. With the exception of gravitational/tidal and nuclear energy, including geothermal energy, all the energy sources that are today designated as renewable are either directly or indirectly entering the Earth system as electromagnetic radiation from the Sun. The source of the Sun's radiation is nuclear energy that is now also available on Earth in forms of fission and fusion. As will be discussed in later chapters, these terrestrial energy sources can also, to a large extent, be considered renewable and sustainable. By measuring the radiation hitting the Earth's surface, we can measure the incoming energy to the Earth system. Since the Sun will continue to radiate until long after the Earth has been swallowed by the Sun's increasing radius, we can regard the Sun as an infinite energy source. This means that there is no physical limit to the amount of energy we can use on Earth if we do not care whether or not it is sustainable. We also have the technology to measure the electromagnetic radiation leaving the Earth, and by combining this, we can calculate the energy balance of the Earth system. The second law of thermodynamics tells us there is a direct relationship between the energy entering or leaving a system, and the system's temperature and entropy change. Since we can readily measure the temperature and the radiated energy of both the Sun and the Earth, we can use this to find the change in entropy of the Earth. The relation is simple enough:

$$dS = \frac{dQ}{T} \quad , \tag{4.29}$$

where dS is entropy change, dQ is heat (in this case in the form of electromagnetic radiation) entering or leaving the system, and T is the temperature of the system. The equal sign in the equation (4.29) is only applicable for a theoretical, closed system. Any system where there is an exchange of energy, material or both with the environment of the system is not closed, and the equal sign must be changed with a difference. All real, physical systems are not closed, and the Earth-Sun system is no exception. This means that the entropy of the Earth must either increase or decrease. By using equation (4.29) we can calculate which is the case. By studying the history of the Earth, we see that all three phases of water have existed through most of the planet's life time [2]. This means that the temperature of the Earth must have been stable within the range where this is possible. We can therefore conclude that the incoming radiation from the Sun, dQ_{Sun}, and the outgoing radiation from the Earth, dQ_{Earth}, must be approximately equal, $dQ_{Sun} \approx dQ_{Earth} = dQ$. The measured temperatures of the Sun and the Earth are $T_{Sun} \approx 6000K$ and $T_{Earth} \approx 300K$ [2], and by inserting these and combining the respective expressions of equation (4.29) for the Sun and the Earth, keeping in mind equation (4.2) we find

$$dS_{Earth} = \frac{dQ}{T_{Sun}} - \frac{dQ}{T_{Earth}} < 0 \quad . \tag{4.30}$$

We see by this that the entropy of the Earth is decreasing. The question to be asked is then how we can account for this entropy decrease. As has been mentioned several times in this chapter, a decrease in entropy is the same as an increase in complexity. In

accordance with Schrödinger's definition of life, the decreasing entropy of the Earth can be attributed to life on Earth or technical development. Live structures keep themselves alive by building more complex structures from less complex structures, which can be seen as draining the Earth of entropy [1]. Since the entropy of the Earth system is decreasing, we can argue that the Earth is a living system based on Schrödinger's definition of life. *In order to have sustainable development on Earth, we must then ensure that it's entropy keeps decreasing.* We can then call this 'Schrödinger's definition of sustainable development', and it includes all efforts made by humans that leads to a decrease of the entropy of the Earth. This will then include all processes that cause an increase in complexity, and exclude any form of combustion and other processes that leads to a higher level of disorder, meaning a higher entropy. In the context of this thesis we are interested in the entropy contribution attributed to our different methods for generating energy, especially electric energy. In the next chapter we will examine different energy sources, and analyze whether or not generating usable energy from them is in the direction of sustainable development based on Schrödinger's definition.

CHAPTER 5

Energy Sources

In this chapter, we will go through the conventional energy sources used today, where each energy source will be treated in its own section. Based on the definition given by Schrödinger [1] [11], we will analyze the sustainability of each energy source by estimating the amount of waste heat and entropy produced by the energy production from each source. We can find this waste by looking at the ratio between the available energy in a source and the useful energy extracted, since all energy loss can eventually be approximated as heat, radiated at ambient temperature. In order to do this, some basic theoretical tools are needed that are common for many of the production methods. We will therefore introduce this chapter with a short presentation of these tools (that have not already been introduced in chapter 4), as well as some terms. Because the monetary cost of utilizing an energy source is dependent on factors that are not purely physical, such as political subsidizing and transport method of the source, we will not do an analysis on how much money it would cost to extract energy from the different sources.

Primary energy is the energy that is embodied in an energy source as it exists in nature. This can be the energy released in a nuclear reaction, the energy of electromagnetic radiation from the Sun or the potential energy in a water magazine [8]. Using a large variety of technology, humans convert this primary energy into secondary energy that is usable in everything from heating to electrical appliances. Secondary energy is therefore electricity, different forms of fuel such as gasoline and ethanol, gas etc. [8]. Even though we use the term 'energy production' we are never able to produce energy. From the concept of energy conservation, we know that energy can only be transformed from one form to another, never created or destroyed. In an ideal, hypothetical system, this energy conversion could be 100 % efficient. However, in any real system there will always be some form of friction, viscosity, turbulence or other process that causes an energy loss, which again produce an entropy gain. We generally differentiate between mechanical and thermal energy. Mechanical energy refers to any kind of energy that does not involve any

heat exchange, such as electrical energy, the potential energy of an object at a height and kinetic energy. Thermal energy results from burning any kind of fuel, such as fossil fuels, biofuels or fissionable material. The conversion efficiency from thermal to mechanical energy is limited by the *Carnot efficiency*, which will be derived later in this chapter. The entropy production caused by the dissipated energy can be estimated using the relation

$$dS = \frac{dQ}{T} \ . \tag{5.1}$$

This is the same equation used in section 4.4 where we used it to calculate the entropy balance in the Earth-Sun system. When we want to find the entropy production from the energy loss, we let dQ be the energy loss, and T be the ambient temperature.

Many thermal energy production methods utilize a steam cycle or some other form of heat engine. A very simplified sketch of a steam cycle is presented in figure 5.1.

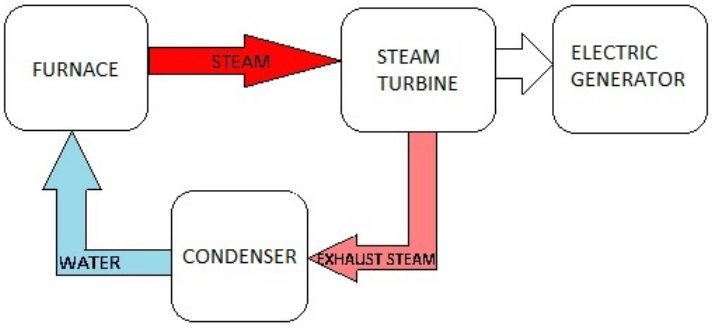

Figure 5.1: A heat source is used to transform water into steam that drives a turbine powering an electric generator. The exhaust steam is compressed and reheated by the heat source to be used again.

Since thermal energy is a lower grade of energy than mechanical energy, the transformation from heat to electricity will involve a significant energy loss. The efficiency of a heat engine is dependent on its design, but a theoretical maximum efficiency of any heat engine is given through the Carnot efficiency. The Carnot cycle is a well known thermodynamic concept that sets an absolute theoretical maximum efficiency on the energy conversion from thermal energy to work in a heat engine. It can be expressed graphically in a TS diagram where the state of the system is expressed as a point on a graph with temperature on the vertical and entropy on the horizontal axis, see figure 5.2.

The Carnot cycle is a reversible cycle, meaning that the entropy is conserved in the full cycle. This can be used to calculate the total work done by the heat engine. The Carnot cycle consists of four steps: first, a reversible isothermal expansion of the working fluid; second, an isentropic expansion meaning a reversible adiabatic expansion; third, a reversible isothermal compression of the working fluid, until finally an isentropic compression leads the working fluid back to its original point of thermodynamic values. During the first isothermal expansion, heat is absorbed from the hot reservoir and leads to an

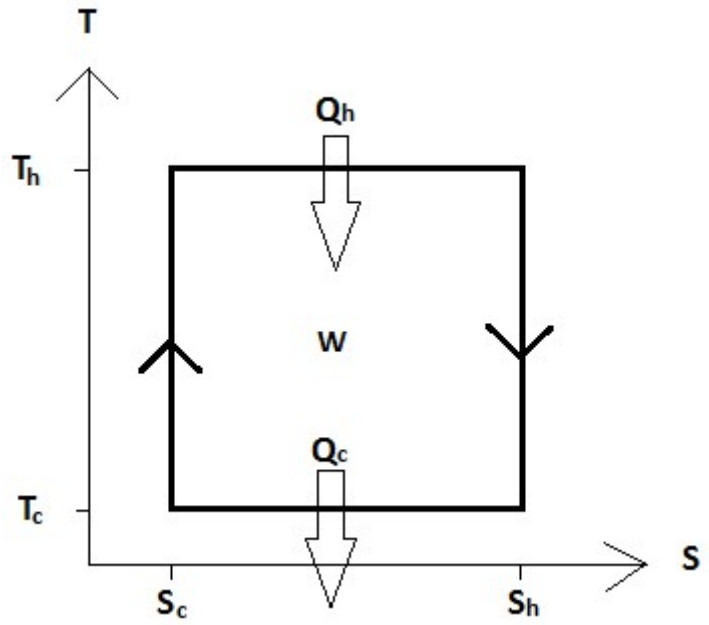

Figure 5.2: A simple TS diagram of the Carnot cycle.

increase in the entropy of the working fluid by an amount

$$\Delta S_1 = \frac{Q_h}{T_h} \tag{5.2}$$

where T_h is the temperature of the hot reservoir. During the isentropic expansion, the entropy is conserved and the temperature is decreased to the value of the cold reservoir, T_c. Since there is no heat exchange during this expansion, the temperature decrease is accounted for by the engine doing mechanical work on its surroundings. Next, during the isothermal compression, the entropy of the gas is decreased by an amount

$$\Delta S_2 = \frac{Q_c}{T_c} \tag{5.3}$$

During the last stage, the temperature is raised to T_h again and the entropy is conserved. Since the entropy is conserved in the complete cycle, we know that $\Delta S_1 = \Delta S_2$, and therefore that

$$\frac{Q_h}{T_h} = \frac{Q_c}{T_c} \quad . \tag{5.4}$$

Since the energy must be conserved, we can write $Q_h = Q_c + W$ where W is the work done by the heat engine. The efficiency of the engine is the ratio of the useful energy output and the required energy input, $e = \frac{W}{Q_h}$. Combining these equations lets us write the efficiency as $e = 1 - \frac{Q_c}{Q_h}$, and with some algebra we arrive at the desired expression

$$e = 1 - \frac{T_c}{T_h} \quad . \tag{5.5}$$

This is the efficiency of a Carnot engine. The equality is due to the cycle being reversible. Since all natural processes are irreversible, the real efficiency of any heat engine will always

be lower than the theoretical Carnot efficiency of that engine. By combining equations (5.2) and (5.3) we can turn the energy conservation around and express the work done by the engine as a function of the entropy and temperature changes at different stages of the cycle

$$W = Q_h - Q_c = \Delta S_1 T_h - \Delta S_2 T_c = \Delta S(T_h - T_c) \quad , \tag{5.6}$$

where ΔS is the difference between the highest and lowest entropy value of the system. Brillouin characterized a closed systems possibility of performing mechanical or electrical work as negentropy [17]. In a heat engine, this negentropy is contained in the temperature difference between the two reservoirs, but as he states, it can also be due to a difference in pressure or electrical potential.

5.1 Gravitational power

The gravitational force exerted on the Earth by both the Moon and the Sun causes the surface of the Earth to shift. We observe this easily in the tidal motions of the Earth's oceans. The idea of generating electricity from the energy of the tides has been pursued for some time, and can be done in two main ways. One way is to extract the potential energy in the head of water by creating tidal barrages or lagoons. This involves closing off an estuary with a damn, or building a bounded reservoir inside an estuary, respectively. The trapped water would then be channeled through a turbine, similarly to the concept in hydro power [26]. The other approach is to extract the kinetic energy in the horizontal tidal flows by constructing current turbines immersed directly in the flow [26]. Even though tidal energy is cyclic, and therefore an intermittent energy source, the tidal cycle is regular and well understood. This means we can predict, and in many cases compensate, for the variability in the production. In this way it differs from other intermittent sources, such as wind and solar power, where the production is affected by relatively unpredictable weather phenomena such as wind speed and clouds.

One of the largest barrages constructed is the La Range barrage in France, which has a total installed capacity of 240 MW [26]. As will be further discussed in the section about hydro power, the efficiency of power production using a barrage will depend on the height difference between the water on each side of the barrage. This is equivalent to the height of the fall in a hydro power facility. The difference between high and low tide shows great variability on different locations on Earth, and different areas will therefore be more suited for power production from tidal energy.

Generating electricity from the potential energy of the trapped tidal water using barrages or lagoons does not in itself involve powering a heat engine, but is mechanical work. The principal entropy production is therefore absent in this case. However, since this method of energy production involves two major production periods without the possibility of extraction between them, many barrages and lagoons are connected to some form of energy storage system. These can involve driving a heat engine or powering an electrolysis

production of hydrogen [26]. This will involve a principle or configurational entropy production respectively.

As will be further elaborated in the subsection about wind power, placing current turbines directly in the tidal flow will lead to entropy production through energy dispersion caused by the creation of turbulence in the flow. Since the particles in a fluid have a shorter mean free path than in a gas because of the higher fluid density, this effect will be more prominent for wind turbines than water turbines. The same arguments about the principle entropy production hold for water turbines as for barrages and lagoons. However, some turbine designs in Scotland utilize a technology called Tidal Delay, which uses energy from the water turbines to power a heat store, generating steam [26]. While this tackles the problem of the cyclic availability of tidal energy, it will lead to principal entropy production that can be estimated using Carnot's law, in addition to the entropy increase caused by the turbulence.

5.2 Geothermal Energy

The Earth is heated from the inside because of nuclear decay from naturally occurring radioactive isotopes at large depths. In this respect, geothermal energy can be seen as a form of nuclear energy. In a geothermal power station, cold working fluid is pumped through pipes drilled into the Earth, where it is heated and pumped back up to drive a heat engine. The availability of geothermal energy is therefore highly dependent on the location, depth and temperature gradient of the hot reservoir. Some locations are more suited for geothermal power stations because natural geological processes bring the hot material closer to the surface. Also, if the source of the heat in the hot reservoir is not stable, the artificial cooling caused by the extraction of heat to the power station will eventually cool the reservoir and render it useless. Building a power station in such areas can therefore prove to not be commercially viable.

In order to calculate the total efficiency of a geothermal power station, we need to know how efficiently the heat is extracted from the hot reservoir and the conversion efficiency of the heat to electricity. Many different designs of geothermal power stations exist that use different working fluids, and they will of course have different efficiencies [20]. However, we can estimate the theoretical maximum efficiency of a geothermal power station by assuming that the hot reservoir and the working fluid reaches thermodynamic equilibrium, and then find the Carnot efficiency of the power station using equation (5.5). The high temperature reservoirs are most suited for electricity generation, and have temperatures of $> 220^oC$ [20]. If we assume the cold reservoir has room temperature (reaching a lower temperature would require energy to cool the reservoir which would lower the efficiency of the power station), the Carnot efficiency becomes

$$e = 1 - \frac{300K}{593K} = 0.5 \ . \tag{5.7}$$

Like any form of thermal energy production, geothermal energy increases the entropy of the Earth through dissipation of heat. By heating and cooling the working fluid the

entropy will vary with an amount ΔS_1 and ΔS_2, which gives the work done by the generator in accordance with equation (5.6). As we see from the Carnot efficiency, about half of the primary energy in the geothermal well is dissipated to waste heat. The typical installed capacities of the three main types of geothermal plants are about 5 MW for small plants, 30 MW per unit for medium plants, and 45 MW per unit for large plants [8]. By equation (5.1), these then generate a principle entropy production rate per second of 17 kJ/K, 100 kJ/K and 150 kJ/K respectively, if we let T = 300 K.

Since there is no combustion process, geothermal energy does not affect the configurational entropy. The thermodynamical entropy will increase, which will lead to an increase of the Earth's entropy, and geothermal energy is therefore not completely sustainable in Schrödinger's definition.

5.3 Hydro power

Hydro power is a collective term for all forms of power production using water as the driver of the power plant. Hydro power plants take advantage of the potential energy in falling water through the relation $E = mgh$, where m is the mass of the falling water, g is the gravitational acceleration and h is the height of the fall. As we see, their power production capacity is therefore strongly dependent on the height of the fall. The primary power in the falling water can be estimated as $p = mgh/t = \rho \dot{V} gh$, where ρ and $\dot{V}$ are the water density and volume flow rate respectively [3]. Two main types of power plants are in use, regulateable and intermittent (run-of-the-river) plants [3]. Regulateable plants include water dams and magazines where water can be stored in periods of heavy precipitation and low electricity spending. This also makes the hydro power plants useful in periods of heavy rainfall and snow melting or dry periods, since they can store water for long periods, i.e. several months, and regulate the water flow to the connecting rivers [4]. Regulateable plants include both pumped storage hydro power and conventional hydro power. Pumped storage power plants differ from conventional hydro power plants in that they can use electric pumps to raise the water back up into the high located magazine in periods of excess electricity [3]. This is highly advantageous as energy production and storage is then included in one and the same structure. Furthermore, in addition to being able to deliver base load energy, we can regulate the water energy production according to the energy demand. This enables regulateable hydro power to compensate for intermittent energy sources, such as solar and wind energy, as well as producing topping power for other constant power production methods such as nuclear energy.

The efficiency of a hydro power plant will vary depending on location and turbine design. The three main types of turbines used for power generation are the Francis turbine, the Pelton turbine and the Kaplan turbine, which all have different operational configurations where their efficiency is maximized [3]. In general, the Pelton turbine is optimized for low flow rates and large heights (usually 450 m or higher), the Kaplan turbine for low heights and a medium flow rate, while the Francis turbine performs best in areas of medium height and high flow rate [3] [36]. Since the conversion from primary to secondary energy in hydro power is conversion between two types of mechanical energy, the conversion

efficiency could in theory almost 100%. This is not the case of course, since there will always be sources of energy loss such as friction. Both the Pelton and the Francis turbines are usually able to extract between 90 to 95% of the primary energy in the water [36]. The efficiency of the Kaplan turbine is very dependent on the actual water flow compared to the design rating, but the efficiency of the power plant is usually stable since it is common to install several turbines in parallel [36].

Hydro power is mechanical energy and does not involve any heating and cooling processes. The principal entropy production then disappears, as well as the configurational entropy by the same arguments as in the previous section. The water is led through pipes, and the dissipative entropy creation is therefore also minimal. As mentioned earlier, the conversion efficiency of hydro power is in the range of 90 - 95%. A 10 MW hydro power plant (often considered the capacity limit between large and small hydro power [36]) has, with a 90% conversion efficiency, a loss of 1 MW, and would then by equation (5.1) only have an entropy production rate per second of 3.3 kJ/K for T = 300 K. The large Itaipu pant on the border between Brazil and Paraguay has a capacity of 740 MW [36] and has then an entropy production rate per second of 723 kJ/K. If the construction of the hydro power plant involves creating a magazine in an area that previously contained forest or other vegetation it can be argued that the destruction of this contributes to an increase in the configurational entropy of the Earth. However, many of the water magazines are located in high areas of little forestation, and many living organisms thrive in the habitat provided by the magazine, making this contribution negligible if not even contributing to an increase in complexity.

5.4 Solar Power

With the exception of gravitational (tidal), geothermal and nuclear energy, all other renewable energy production methods can be considered a derivative of solar energy. This section will treat production methods that directly convert solar radiation into energy. Depending on the location and time of day, the Earth's surface is hit with about 1 kW/m^2 solar radiation. It is here assumed that no clouds or other form of atmospheric pollutant blocks the way of the radiation [3]. In comparison, about 1.4 kW/m^2 hits the top of the Earth's atmosphere. The difference in these is either reflected or absorbed by the atmosphere. These numbers will obviously vary depending on the time of year, the solar sunspot cycle and the angle at which the radiation hits the collection point. The two first uncertainties only affect the number between ± 0.04 and 0.3 %, while the angle will be much more relevant [3]. In addition to these factors, the amount of available solar radiation to be collected at a certain location on the Earth's surface will depend on the degree of cloudiness, the extent of atmospheric absorption and in particular the number of hours of daylight at a given time of the year, which will depend on the latitude and the solar declination at the particular location and particular day of the year [3]. By these arguments, it is clear that solar power is a highly intermittent energy source, and it's efficiency will be very dependent on the location of the solar farm.

There are two main types of solar power production methods; solar thermal and pho-

tovoltaic. Some hybrid designs that try to combine these two collection methods also exist [22], but will not be considered here. Solar thermal can be used for direct heating (e.g. by transporting the heat with water), or by converting the heat to electric or other mechanical energy. Several different designs for the solar collectors are already being constructed or have been suggested, all with particular optimal operational conditions and purposes [22]. They will have different efficiencies, but we can find their maximum efficiency by assuming perfect conditions and using the Carnot efficiency.

Photovoltaic is used to directly produce electricity without having to convert from heat to electric energy, and the efficiency can therefore not be estimated using Carnot's equation. Apart from the already mentioned limiting factors such as the incident angle of the solar radiation and the total solar irradiance, the temperature of the photovoltaic cells have a significant impact on the conversion efficiency [21]. This means that, even though the intensity of the solar radiation hitting the Earth is much higher closer to the equator than it is closer to the poles, the difference in efficiency is not necessarily as affected since the temperature usually also decrease as we move away from the equator. To calculate the efficiency of a photovoltaic cell, we can find the ratio between the power density of the cell and of the solar irradiance. Typical values of photovoltaic power densities are $4 - 10W/m^2$ [7], and assuming the solar irradiance is 1 kW/m^2 this gives us an efficiency of $0.4 - 1.0\%$. Since all the radiation hitting the area where the panels are placed would either be absorbed or reflected regardless of the existence of the panels, the fact that they do not convert a large amount of the radiation into electricity does not contribute to an additional entropy increase through dissipation. On the other hand, when the solar radiation is absorbed by plants, substantial entropy decrease takes place due to the buildup of complexity. The entropy contribution of solar panels will therefore be highly dependent on the original landscape on which they are placed.

It is of interest to compare the efficiency of energy conversion between solar energy and photosynthesis. This is because solar panels are often placed in areas where there could otherwise have been vegetation. In the interest of sustainable development from Schrödinger's perspective, the buildup of complexity that results from photosynthesis is more valuable than the energy conversion to electricity. If the land in question would be suited for agriculture, complex plant material could again be used as food for even more complex organisms. For the most productive terrestrial ecosystems, such as forests, the conversion efficiency of the photosynthesis is about 1.5%, while it is no more than 0.3 % on a global scale [23]. Comparing this with the range of efficiencies of photovoltaic solar panels, we see that, depending on the original vegetation in the area where they are placed, photovoltaic cells might increase or decrease the amount of absorbed solar radiation. If the solar panels (both photovoltaic and thermal) are placed in areas where there otherwise would not be any vegetation, such as on buildings, parking lots, roads or in the desert, they would not hinder the buildup of complexity on Earth, and would therefore not increase the configurational entropy. In that case, solar power is sustainable in Schrödinger's definition.

5.5 Wind Power

Wind turbines utilize the kinetic energy in wind to generate electricity. From fundamental physics, it is clear that it would be impossible to have a 100% efficient wind turbine, because this would mean that all the kinetic energy of the air particles would be absorbed. This would lead to a buildup of particles behind the turbine, making it impossible for more wind to pass through. The theoretical max value of the power efficiency of a wind turbine is called the Betz limit, which has the value $C_p = 0.593$ [3]. Common real values for the efficiency are between 0.4 and 0.5 [3], meaning that the leftover 50 - 60 % of the wind power is dissipated through turbulence generated by the motion of the turbine. The power that can be extracted from the wind by a wind turbine is given by

$$p = C_p p_{wind} = (1/2) C_p A \rho v^3 \quad , \tag{5.8}$$

where v is the wind speed, A is the area of incident wind (i.e. the area swept by the wind turbine) and ρ is the density of the air [3]. Since wind power is dependent on the wind speed, it is a highly intermittent production method. In most cases, production of wind power relies on other forms of power production that can act as replacements in periods of little wind in order to be able to deliver base load energy. Depending on what source this energy comes from, installing wind power could actually lead to a higher emission of green house gases and other pollutants [3]. 7 power classes exist when considering wind power production, see table 5.1.

Power class	Wind power (W/m^2)	Speed (m/s)
1	<200	<5.6
2	200 - 300	5.6 - 6.4
3	300 - 400	6.4 - 7.0
4	400 - 500	7.0 - 7.5
5	500 - 600	7.5 - 8.0
6	600 - 800	8.0 - 8.8
7	>800	>8.8

Table 5.1: The 7 wind power classes with corresponding wind power and wind speed values. Recreated from [3]

These power classes are used to determine whether or not an area is suited for wind power production. If the power class is less than 3, it is usually not commercially viable to have a wind farm in that area. Since the power production of a wind turbine is dependent on the wind speed, it is easy to think that higher wind speeds means more electricity generated. However, because of the risk of damage, wind turbines are turned off when the wind speed exceeds $25\,m/s$. This means that wind parks typically only produce electricity when the wind speeds are between $4 - 25\,m/s$ [3].

While it is true that wind energy does not produce any greenhouse gases while operating, large amounts of energy and materials are required to build each turbine. In a 300

MW wind power installation consisting of 152 wind turbines of 2MW requires 930 000 m^3 of concrete [7]. Scaling this to a 1000 MW installation would require 3 100 000 m^3 of concrete. If the wind turbine is of the type that utilizes a permanent induction generator it may also use 2000 kg of neodymium-based permanent magnet material, where neodymium is a rare earth material [7]. Other such rare earth materials utilized in wind turbines are Dysprosium, Praseodymium and Terbium for magnetic properties, and Chromium, Nickel, Molybdenum and Manganese for corrosion resistant components. Several of these are also used in solar panels and hydro power facilities [7]. In addition to the concerns about toxicity and environmental damage from extracting processes, there is also the more political concern that over 90% of the rare earth supplies originates from China alone [7].

Considering the sustainability of wind power we must look at the entropy contribution to Earth. The motion of the rotor is a source of great turbulence in the air, causing entropy increase through energy dissipation. Unlike the case for hydro power where the rotors are located in closed pipes, this turbulent air is released in free space. If we approximate the energy dissipation from turbulence as heat, we can estimate the entropy production using equation (5.1), letting dQ be the nominal maximum energy of the turbine production and T be room temperature. Wind turbines usually produce rated or maximum power when wind speeds are around $14\,m/s$ [3], and using equation (5.8) this gives us $p = 15.1MW$ for a rotor diameter of $100\,m$ and air density of $1.18\,kg/m^3$. This would give an entropy production rate of $dS = 50.3\,kJ/K$ using equation (5.1) and $T = 300K$ (it should be noted here, that the largest onshore wind turbines today only have power ratings of about 6 MW). In order to ensure the least amount of turbulence in the air entering the rotor area, the surrounding area must be leveled [3]. Also, since the rotor blades are produced in full size at a factory not located in the park, roads wide and open enough to facilitate transport of these blades must be built in the park area. Unless the wind turbines are placed offshore, this means that large areas of forest and other vegetation must be removed. This is not contributing to sustainable development from Schrödinger's perspective. With this in mind, in addition to the entropy production from dissipation, the low energy density of a wind park ($0.5 - 1.5W/m^2$ [7]), its intermittent nature, and the negative impacts on bird life and on people living in close proximity of the wind parks [7], the substantial public and governmental support of wind power can be difficult to understand.

5.6 Energy from biofuels

During the course of a year, the surface of the Earth is hit with $3.8 \times 10^{24} J$ of solar energy, of which a small percentage is converted into plant matter through photosynthesis [3]. Biofuels are produced from biomass, which consists of living or dead plant or animal matter, the wastes from such organisms and the waste of society that has been created by such organisms [3]. The term *bioenergy* is used to describe the stored chemical energy in biomass. Biofuels are used in both electricity and heat production, but the main use of biofuels in the developed world is for transportation [3]. The two most common biofuels

are bioethanol and biodiesel, and their usage has increased substantially the last 40 years [3].

Producing electricity from biofuels will contribute an emission of CO_2 to the atmosphere of 220 $g/kWh(e)$ per year [7]. Emissions of SO_2 and NO_2 gases are also considerably higher from biofuels (and fossil) than from any other designated renewable energy source [7].

Biological materials are highly complex, low entropy materials. Therefore, burning them and reducing them to their elementary constituents leads to a tremendous entropy production e.g. from about $10^{-10000} J/K$ to $10^5 J/K$ for 1 kg material [1]. In the interest of sustainable development, biological material should be used as food, feed or eventually as fertilizer in order to develop even more complex materials. If most of the biological material is used for processes contributing to development, and only the unusable remainder is converted to biofuel and burned, their use may be acceptable, but this evaluation, based on Schrödinger's definition of sustainable development, is not considered up to now. In counties such as the USA and Brazil, large amounts of bioethanol are created for the transport section using either corn or sugar cane as feed stock [3]. In this and similar situations, where land area and produce that could be used for food production are being used for growing biofuel feed stock, we can conclude that the use of bioduels are highly unsustainable in Schrödinger's definition.

5.7 Fossil Energy

More than 85 % of the primary energy production in the world originates from fossil fuels [6]. We can make the same arguments about complexity reduction for all fossil energy sources as we did for biological material in the previous section. However, with the exception of burning wood (which technically can be considered a biofuel), the configurational entropy generating processes have already occurred naturally when the fossil energy source is extracted from the Earth. Burning fossil fuels therefore makes only a minor contribution to the configurational entropy.

Because coal power plants are able to deliver continuous electricity from remote locations, coal is the fossil fuel source that is most often used to produce electricity [9]. Since the production is continuous, and fuel is easily available at a relatively low cost, coal power plants are able to deliver base load electricity. Electricity is produced from coal via a steam cycle, which has, from thermodynamics, an efficiency of about 35-40% [9]. When burning coal, large amounts of CO_2 are produced, as well as other gases such as sulfur dioxide, nitrous oxide, oxides of mercury, and fly ash because of impurities in the coal. In addition, a small amount of radioactive isotopes contained in natural coal is released upon burning, leading coal power plants to release more radiation than a nuclear power plant [9]. Although the amount of radiation is still not cause for concern about public health [9], it is interesting from the perspective on public opinion towards the dangers of fossil and nuclear power production. The capacity of a typical coal power plant is 1 GW. With an efficiency of 40%, this leads to a principal entropy production rate per second of 5 MJ/K.

Another common fossil energy source is natural gas, which consists mainly of methane (CH_4), which is used for both domestic heating and electricity generation. The efficiency of a typical gas powered plant is between 50-60% [9], which for a capacity of 1 GW gives an entropy production rate per second of 2.2 MJ/K through equation (5.1). In addition to having a lower principal entropy production, natural gas also emits less CO_2 and other toxins than coal fired plants [9]. When natural gas is used as a source of heating, it can be argued that the efficiency is close to 100% since the heat in this case is the desired result instead of a loss.

Oil (petroleum) is not commonly used in electricity generation, rather as a transport fuel and for heating purposes [9]. Gasoline and diesel are two common transport fuels that can be extracted from petroleum through fractional distillation [3]. The Carnot efficiency of a typical gasoline powered car engine is about 55%, and the real efficiency is usually below 40% [37]. This tells us that about 60% of the energy in the fuel is lost as heat, contributing to a principal entropy production.

5.8 Nuclear Power

Nuclear power refers to the production of electricity from the controlled splitting of heavy atomic nuclei or the combination of light ones. This is called fission and fusion respectively and will be treated separately here. Both reaction types take advantage of the difference in binding energy between the reactants and the product. The binding energy is defined through Einstein's famous relation $E = mc^2$, and can be expressed as follows

$$E_B = (Nm_n + Zm_p - m_A)c^2 \quad , \tag{5.9}$$

where N is the number of neutrons in the nucleus, Z is the number of protons and m_n, m_p and m_A are the masses of a neutron, a proton and the nucleus respectively.

As can be seen in figure 5.3 for nuclei lighter than Fe (iron), the binding energy is larger in the reactants than in the products, while the opposite is true for nuclei heavier than Fe. This is why fusion gives a positive energy output for light nuclei, and fission for heavy nuclei. The energy release in both fission and fusion reactions is in the order of MeV per nucleon, which is six orders of magnitude larger than that of chemical reactions per atom [5].

5.8.1 Fission

The most common nuclear power plants existing today are fission plants using the Uranium isotope U^{235} as fuel to power a steam cycle. These power plants are capable of generating base load electricity on a large scale without producing any CO_2 or other greenhouse gas emissions [9]. Even though the U^{235} isotope is far less common in nature than U^{238}, the known reserves are still large enough to sustain current levels of power production for several hundred years [9]. However, the spent fuel rods of U^{235} contain large amounts of U^{238} that can be used to breed the plutonium isotope Pu^{239}, which is

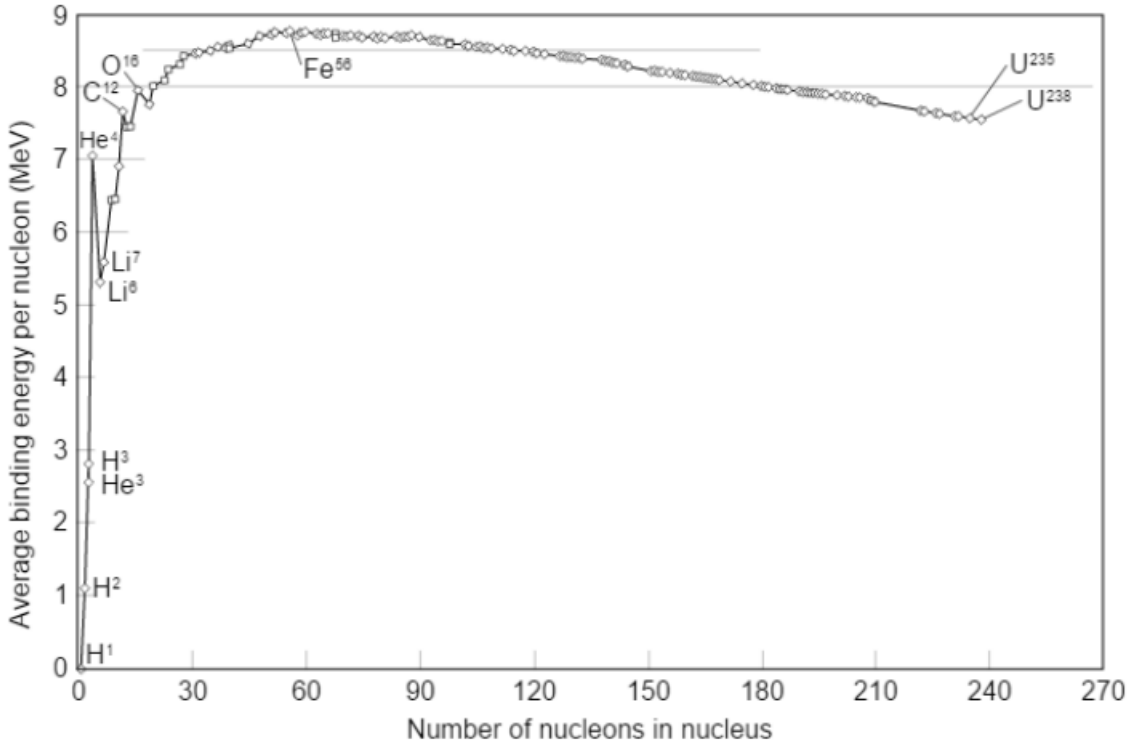

Figure 5.3: A simple plot of the binding energy per nucleon vs the number of nucleons in the core. The figure is found online, but checked against [31].

also a suitable fuel for fission. This plutonium can also be used in a 'breeder' reactor to produce more plutonium than is being consumed and thereby increasing the usable fission fuel substantially. If such breeder reactors are being used, the fuel reserves could last for several thousands of years [9].

Fission is by definition splitting more complex molecules into molecules of less complexity, and therefore contributing to a reduction of the total complexity, causing an increase in the configurational entropy. However, if breeding reactors are used, fission becomes more sustainable from Schrödingers perspective, since plutonium has a higher mass number than uranium. Nuclear energy can have a power density of up to $4000\,W/m^2$, which is as mentioned earlier far higher than any energy source based on chemical reactions [7]. Since the energy released in the nuclear splitting is used to power a heat engine, the principal entropy will increase with an amount we can estimate using Carnot's law.

A common design of nuclear reactors are the VVER type reactors, which are used by many different countries [28]. As an example of the efficiency of nuclear fission, we can take a closer look at the VVER-1000 reactor. It has a reactor thermal output of 3000 MW, producing a unit electric power of 1040 MW [28]. This gives a conversion efficiency from thermal to electric power of 0.35. The rest of the thermal energy is the source of entropy production, which we can estimate using equation (5.1). The temperature of the exhaust from a nuclear reactor is usually only about 10-20 degrees higher than ambient temperatures, so we can use $T = 300K$ in our estimate. This gives a principal entropy production rate of 6.5 MJ/K.

5.8.2 Fusion

In a fusion reactor, we want to replicate the process driving the Sun. In the solar core, the temperature and pressure is high enough that p+p reactions can take place, eventualy forming helium cores consisting of two protons and two neutrons. Replicating this exact reaction path would not be commercially viable since the creation of neutrons from protons would require a large energy input. Instead, current developments in fusion reactors focus on the hydrogen isotopes *deuterium* (D) and *tritium* (T), which already contain neutrons, as fuel. These reactions have a 10^{24} times higher reaction rate than the p+p reactions in the solar core [6]. The specific DT reaction of interest is the following:

$$\mathrm{D} + \mathrm{T} \rightarrow {}^{4}\mathrm{He} + \mathrm{n}.$$

The two end products have an energy of 3.5 MeV and 14.1 MeV respectively, adding up to 17.6 MeV primary energy released per fusion reaction [6]. Fusion can be used to deliver base load electricity [9]. Compared to other energy sources, fusion power has several advantages. One major advantage is fuel availability. Deuterium occurs naturally in the ocean (ratio D/H = 1/6700 [9]) and can be readily extracted with currently existing technology. The known reserves of the lithium isotope Li^6 (which is what tritium is produced from) are large enough to last 20 000 years without becoming expensive, assuming no major change in energy consumption [9]. Since the energy release in D-D reactions is higher than in D-T reactions it is also assumed that technology will be developed where pure deuterium is used as fuel long before the Li^6 reserves are depleted.

Another advantage is the environmental impact of fusion. It creates no CO_2 or other greenhouse emissions, and the end products of the reaction(s) are not harmful to humans or the planet as a whole. Depending on which fusion reaction is used, the product of the reaction is helium and either neutrons, protons and tritium (which could be reused in other fusion reactions). The helium produced could be used in technology relying on supercooled helium for cooling, such as the superconducting magnets at CERN and in MRI machines. The neutrons that are released in the reaction have high energy and will admittedly activate the surrounding material making it radioactive. However, this is not different from what happens in regular fission reactors today, and the technology for storing this safely is already well established [9]. The radioactive material created is also short lived and would only need to be stored for about 100 years [9] [6]. These neutrinos can also be used to breed more tritium by placing a blanket of Li^6 outside the reactor core. Fusion power is also a very safe form of energy production. Contrary to fission reactors, it is physically impossible to have a meltdown in a fusion reactor due to the small amount of fuel present at any time during the operation of the reactor [9] [6].

In relation to the discussion about sustainability in chapter 4 fusion power is the only means of energy production that is truly sustainable in Schrödinger's definition. The products of a fusion reaction have a higher level of complexity than the reactants and therefore a lower amount of entropy. Although the entire energy production from a fusion reaction as a whole will increase the entropy of the Earth, fusion is the only reaction where the entropy of the fuel decreases as a result of the reaction.

CHAPTER 6

Fusion

This chapter will be a short examination of some of the existing fusion technology that shows promise as a future energy source today. The two main directions in fusion research are magnetic confinement and inertial confinement, and will be treated in two separate sections. Even though the magnetic and inertial confinement fusion technologies are very different, like other forms of nuclear energy they both rely on generating energy to drive a steam cycle [9]. The main difference therefore is not in the power generating aspect, but in the aspect of ignition and confinement of the fuel. The quest for constructing a thermonuclear fusion reactor capable of delivering energy gain has been ongoing for more than half a century [30] [29]. Great progress has been made, but there are still major theoretical and technical difficulties to overcome before fusion energy can be used for power generation [29]. Some of these challenges will be discussed in this chapter, such as overcoming the Coulomb barrier and avoiding the buildup of instabilities, such as Rayleigh-Taylor instabilities.

Both the deuterium and the tritium core involved in a fusion reaction are positively charged ions, and will therefore repel each other because of the Coulomb force. In order to initiate a fusion process, the cores need to be in close enough proximity to each other that their cross sections overlap. The deuterium-tritium cross section is the largest of the fusion cross sections [29], and a larger overlap means a greater probability of fusion. The cross sections of deuterium and tritium are both in the order of a nuclear diameter [9]. The Coulomb barrier needing to be overcome in order for a nuclear reaction to take place is inversely proportional to the distance between the particles, meaning it will increase in strength as the ions move closer. The ions must therefore have a kinetic energy high enough to force the particles close enough together in order for the short range, attractive strong force to become dominant and induce a nuclear reaction [9]. In order for fusion reactions to occur in a deuterium-tritium fuel mix, the temperature must be in the order of 1 keV or higher, which corresponds to about 11.3 million ^oC [29]. This is much

higher than the ionization energy of the deuterium and tritium atoms, and the fusion fuel therefore becomes a completely ionized plasma. In his article from 1957 [30], Lawson discussed how nuclear reactions could be used to power a thermonuclear reactor, and derived some expressions for the power balance of such reactors under various idealized conditions. This lead to the widely used *Lawson criterion*, that is used to estimate how different conditions of the thermonuclear reactor must be in order to deliver a high enough positive energy output. The specific expression for the Lawson criterion differs for the different reactor designs, and some will be mentioned later in this chapter.

6.1 Magnetic Confinement Fusion

In magnetic confinement fusion (MCF), the fuel is confined using complex, interacting magnetic fields. Since the fusion plasma consists of charged ions, they will travel in helical paths along the magnetic field lines due to the Lorentz force, leading to a strong limitation of the ions' ability to move perpendicularly to the field lines [6]. Several different reactor designs have been suggested, such as the spherical tokamak, the reversed field pinch, the spheromak, the field reversed configuration and the levitated dipole [9], but the two most common designs are the *tokamak* and the *stellarator* [6], see figure 6.1. These two designs will be treated in this section.

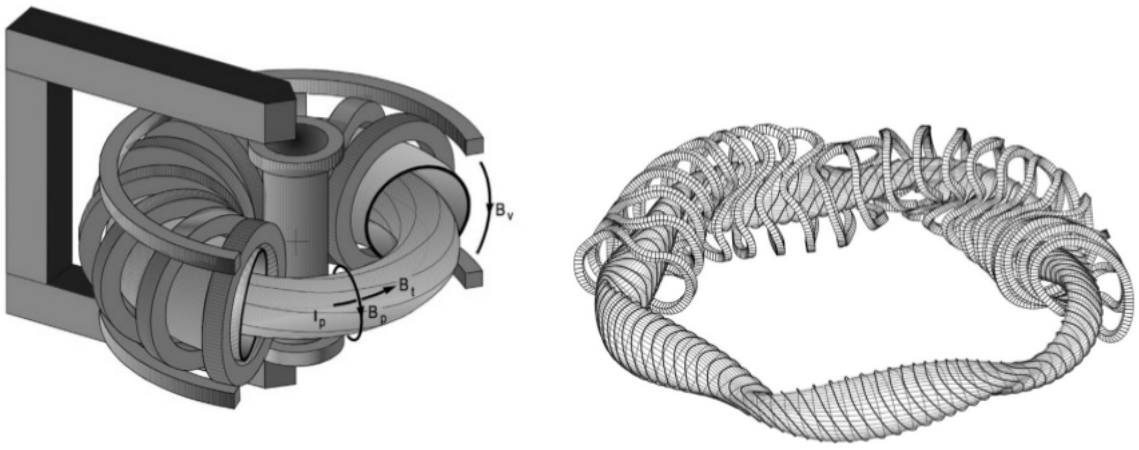

Figure 6.1: The scematic representation of a tokamak and the complex coil system used in a stellarator. Reprinted from[6], Copyright (2016), with permission from Elsevier.

The tokamak is an axisymmetric torus consisting of a toroidally shaped chamber surrounded by coils. The toroidal field coils provide the main toroidal magnetic field (B_t in figure 6.1), and the induced, toroidal current in the conducting plasma chamber itself generates a secondary, poloidal magnetic field (B_p in figure 6.1) [6]. The toroidal magnetic field is strong [9], and the induced toroidal current can, in the largest tokamaks, be up to several million amperes [6]. The toroidal current is induced by an ohmic transformer, where the plasma chamber acts as the secondary winding [6] [9]. The toroidal and the induced poloidal magnetic fields interact and generate a total, helical magnetic field

trapping the plasma particles along the field lines. From basic electromagnetic theory, we know that in order to induce a current in the plasma, the strength of the inducing current to the device must change. The tokamak is therefore a pulsed device, with a steadily increasing supplied current [6]. In order to work as a generator, the tokamak should be a steady state device [9]. Several different designs that aim to provide a fusion device with a continuous production have been suggested, where most of them require some form of external current drive. In a tokamak, a naturally occurring current called 'the boot-strap current' can provide between 0 and 95% of the total current [9], and potentially reducing the need for an external current drive significantly. Unfortunately, achieving a high bootstrap fraction requires a high normalized plasma pressure, requiring structural changes of the tokamak [9].

As mentioned earlier in this chapter, the Lawson criterion is often used to assess the performance of a thermonuclear fusion reactor. In MCF, this criterion relates the product of the pressure and confinement time of the plasma to a temperature dependent function of the plasma, leading to the expression [33]

$$P\tau > f(T) \ . \tag{6.1}$$

This expression is typically considered to be the ignition criterion of MCF. The temperature dependent function has a minimum in the range of $T = 10\,keV$, telling us that for a tokamak the ignition criterion is $P\tau \geq 8.3\,atm\,s$ [33].

The stellarator is another MCF design that aims to provide reactor conditions for a steady state operation [6]. In a stellarator, helical coils are added outside the toroidal plasma [6], and it can be described as a helically symmetric system bent into a torus [9]. The helical coils cause the toroidal magnetic field to twist, eliminating the need for an external current [6]. The three types of magnetic fields required for this twisted shape are a relatively large, axisymmetric toroidal field, a moderately large helical field and a small axisymmetric vertical field [9]. The only net toroidal current in the stellarator is the bootstrap current since it does not contain any external current or ohmic transformer [9]. Since the placement of the helical windings around the plasma ring makes the design of stellarators very complicated, designs aiming at making the construction easier have been suggested. One such design is shown in figure 6.1, where the coils themselves have been twisted in a certain shape, generating a twisted plasma shape [6]. The two main advantages of the stellarator compared to the tokamak are that it is inherently a steady state device and that the plasma is more stable since the toroidal current is small [9]. However, the tokamak design is still favored because it has a much simpler coil system, making them substantially easier to construct [9].

An advantage of the large plasma current in a tokamak, in addition to producing a magnetic field, is that it is a source of ohmic heating because of the resistance of the plasma [6]. Since there is no induced plasma current in the stellerator, other external heat sources are needed to heat the plasma. These might also be necessary in the tokamak after a while, since the plasma resistance decreases steadily with the temperature increase [6]. Examples of such external heating mechanisms are the injection of energetic particle beams of neutral hydrogen or deuterium into the plasma, and the induction of electromagnetic waves into the plasma, favorably with the cyclotron frequency of the plasma

particles [6]. One of the greatest obstacles in MCF is to avoid the buildup of instabilities in the heated plasma, which occur due to the high temperature gradient that must be maintained. As an example of the magnitude of this gradient, the tokamak in the Joint European Torus (JET) in the UK must maintain a gradient of about 100 million ^oC per meter [6].

Globally, several MCF facilities exist where different designs are tested. One of the largest projects is the construction of the tokamak called ITER in France. ITER is short for International Thermonuclear Experimental Reactor, and the project is an international cooperation between Europe, Russia, India, China, Japan, South Korea and the USA [6]. When construction is finished, it is projected that ITER will operate using long pulses of 500 MW fusion power sustained for 400 - 3000 s [6]. In other facilities, such as JET in the UK and JT-60U in Japan, large amounts of fusion energy is already generated in a controlled way, and through the use of scaling laws it is expected that ITER will have even better results [6].

6.2 Inertial Confinement Fusion

In inertial confinement fusion (ICF), the fuel pellet is contained and ignited using the inertia of laser or particle pulses. The idea of using lasers to induce ignition conditions in thermonuclear fusion reactors was first published in 1972 by Nuckolls [29]. The basic concept of ICF is to induce fusion reactions in a small fuel pellet through an initial implosion followed by ignition of the fusion fuel, leading to a final explosion [6]. Several different designs have been proposed for ICF, where the two most common approaches towards achieving ignition are the direct-drive and indirect-drive, see figure 6.2.

In direct-drive, the fuel pellet is hit directly with an array of lasers or ion beams. The fuel pellet is usually spherical, consisting of consecutive layers of deuterium-tritium gas, fuel and an outer ablation layer [6]. In indirect-drive, the spherical fuel pellet is contained inside a cylindrical, metallic hohlraum. Lasers or ion beams are used to irradiate the inner surface of the hohlraum, and the interaction between the metal wall and the beam heats the hohlraum enough to turn it into a plasma. The radiation of this plasma, which peaks in the x-ray part of the electromagnetic spectrum, uniformly irradiates the fuel pellet within [6]. In both direct- and indirect-drive, the fuel pellet has an outer layer of material that ablates easily, called the ablator. When the fuel pellet is irradiated, either directly or indirectly, the outward movement of the vaporizing ablator causes the fuel within to implode. In regular ignition schemes, the confinement time of the imploding fuel is about 1 ns, and densities of about $1\,kg/cm^3$ must be reached in this time in order for sufficient fusion reactions to take place [6].

As mentioned earlier, if high enough temperature and pressure conditions are maintained for some sufficient confinement time, ignition of the fusion fuel will take place, and behave according to the Lawson criterion [30] [29]. The Lawson criterion for ICF can be described through the following relation

$$P\,\tau > \frac{11 f(T)}{\theta_\alpha} \ , \tag{6.2}$$

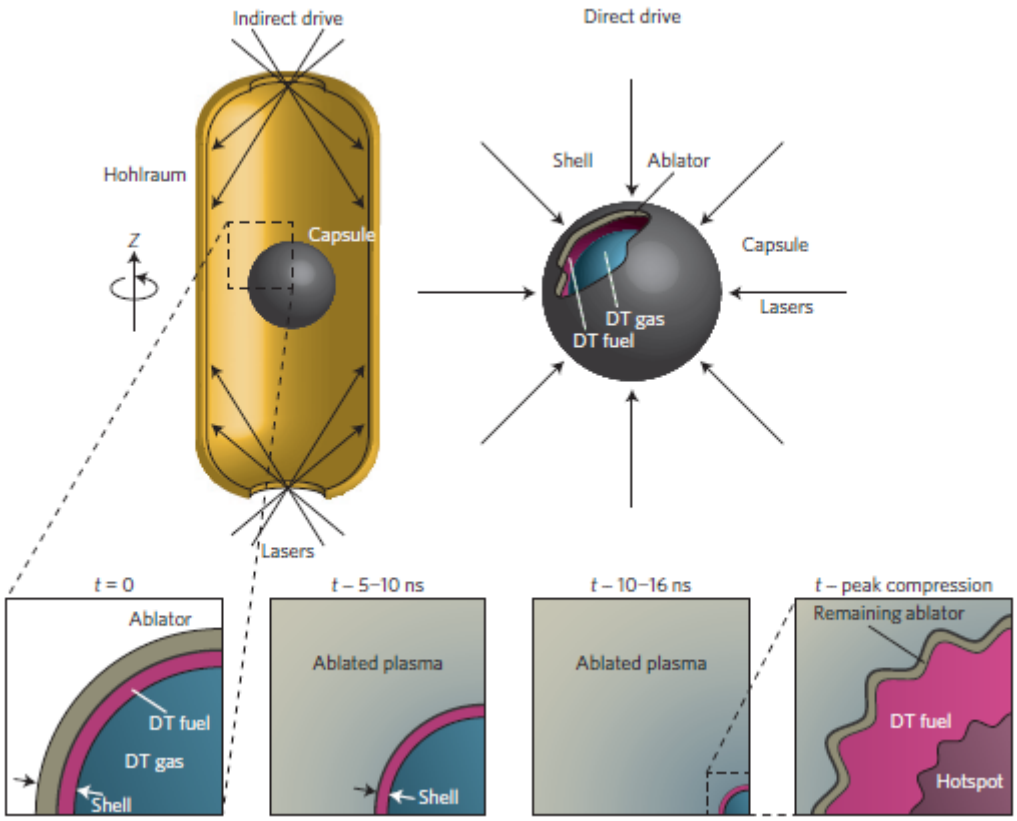

Figure 6.2: From left to right, schematics of the fuel configuration in indirect- and direct-drive ICF. The implosion process is shown for indirect-drive in the bottom four images. Reprinted by permission from Macmillan Publishers Ltd: Nature Physics [29], copyright (2016).

where $P\tau$ is the product of the plasma pressure and the confinement time in seconds, $f(T)$ is a dimensionless function of the temperature, and θ_α is the fraction of α particle energy deposited in the plasma [29]. For plasma temperatures of about $T = 5\,keV$, the function $f(T)$ has the value ≈ 2.6. Assuming the value of θ_α is about 0.8, this gives us the ignition criterion $P\tau \approx 36\,atm\,s$ or higher for ICF [29]. Compared to the ignition criterion for MCF in a tokamak at $T = 10\,keV$ mentioned in the previous section, we see that this is much higher for ICF.

An important factor in the heating of the fusion plasma is the alpha heating. After ignition, a fraction of the alpha particles created will deposit part of their energy into the plasma itself. This heats the plasma further, increasing the fusion rate [29]. Since the input energy needed to reach ignition conditions is very high, the amplification of the reaction rate resulting from the alpha heating is essential for generating a net energy gain from the fusion reaction [29]. The ignition process usually starts in the central core of the fuel pellet, where the hot plasma has a lower density than the dense, compressed shell surrounding it [29]. This is often referred to as the hotspot, as can be seen in figure 6.2. The temperature in the core of an imploding fuel pellet is approximately proportional to the implosion velocity, $T \sim V_{impl.}^{5/4}$ (without the alpha heating), which again is restricted

by the shell hydrodynamic stability [29]. In order to reach ignition then, the fuel pellets are designed in such a way that the inner core reaches a temperature of about 5 keV before ignition occurs. The implosion velocity is in the order of 200 - 400 km/s [33].

As with MCF, several research facilities exist around the globe working towards achieving thermonuclear ignition in ICF targets. One such facility is the National Ignition Facility (NIF) at the Lawrence Livermore National Laboratory in the USA. NIF became operational in 2009, and has as their principle goal "to achieve ignition of a deuteriumtritium (DT) fuel capsule and provide access to HED (high-energy-density) physics regimes needed for experiments related to national security, fusion energy and for broader scientific applications" [35]. Since then, they have been able to achieve laser-fusion implosions with $P\tau$ values above 20 atm s, which is more than half the required energy for ignition [29].

As is the case with MCF, one of the greatest obstacles in ICF is also the buildup of instabilities in the fusion core. One such type of instability is the Rayleigh-Taylor instability, which destroys the spherical symmetry of the implosion. Rayleigh-Taylor instabilities occur in systems where a heavier liquid is on top of a lighter liquid [6] such as is the case in fusion targets. Small nonuniformities in the target are amplified by the hydrodynamic instabilities in the implosion, causing bubble and spike structures to form in the shell outside the hotspot [33]. These instabilities in the shell can penetrate into the hotspot, causing a mixture of the hot fusion fuel with the cold shell and remaining ablator [33] [6]. The following section is a short introduction to a method our team have been working on in order to model the ignition in ICF in an attempt to eliminate build up of Rayleigh-Taylor instabilities.

6.2.1 Using Relativistic Fluid Dynamics in ICF

Today, ignition in ICF is modeled using statistical physics and classic fluid dynamics models. Our team has extended activity in relativistic heavy ion theory, and relativistic fluid dynamics. With Inertial Confinement Fusion (ICF) we aim to extract energy from a highly dynamical, high density plasma of fusion material, such as deuterium-tritium plasma. It is of our opinion that relativistic fluid dynamics, which is used in a part of CERN heavy ion reactions and astrophysics, can and must be used for all high temperature phenomena. It provides a possibility to avoid the Rayleigh-Taylor type of instabilities, which at present are a serious obstacle in ICF. We have worked on modeling rapid ignition and volume ignition in ICF, based on earlier fundamental ideas [24] and its use in ICF [25]. In the course of this thesis, we calculated quantitatively what time extent the igniting laser pulse should have and what absorptivity the fuel pellet should have in order to achieve stable and rapid volume ignition. An article containing these calculations is currently under preparation [34]. The obtained dynamical result resembles qualitatively the 'freeze-out' space-time dynamics of the 'burning' (i.e. hadronization) of the quark gluon plasma in CERN heavy ion reactions. In [24], Csernai showed how a detonation front can have a smooth transition across a hyper-surface with a space-like to a time-like normal vector in exothermic detonations by introducing relativistic considerations. These ideas were studied further in [25] for detonation in ICF in rapid

ignition schemes. It was showed that rapid ignition gives the possibility to have time-like detonation, also called simultaneous volume ignition, where the detonation time is too short for Rayleigh-Taylor instabilities to occur. Further research in this field is needed in order to know if this is a solution to the instability problem in real thermonuclear fusion reactions, and our team has already started planning such activities.

CHAPTER 7

Summary and discussion

As stated in the beginning of this thesis, we know that the standard of living is dependent on the availability of energy. This leads us to conclude that, in order to have sustainable development in general, we must have a sustainable development of the energy production. In this thesis, we have studied an aspect of sustainability that is not often considered, i.e. the inevitable entropy contribution to the Earth all energy producing processes lead to. In chapter 4 of this thesis, we developed the necessary theoretical basis for discussing the entropy of a well defined amount of matter that is independent of the type of matter. This led to the derivation of equation (4.27), that enables us to quantitatively analyze the total entropy of a given amount of matter. This allows us to consider both the kinetic (from thermodynamics) and the configurational (from topology considerations) entropy contribution of the system on the same level, and to compare the entropy content of different types of matter.

Based on the fundamental considerations of Ervin Schrödinger in the context of life and entropy [11], we defined the criterion for sustainability that it must be in the direction of decreasing entropy of the Earth system. Since no real macroscopic process is completely reversible, the increase in principal entropy is inevitable. If we want to have a total entropy decrease, it then means that the configurational entropy must decrease, i.e. that we must have an increase in the complexity. A sustainable energy production method will in this definition have a high efficiency, since all energy loss contributes to the generation of new entropy, and in the best case scenario lead to an increase in complexity. In chapter 5 of this thesis we analyzed the sustainability of different energy production methods based on this definition of sustainability. A summary of these calculations, as well as comments where direct values were not calculated, are presented in table 7.1.

The sustainability of different energy sources are dependent on several different factors, and only the considerations pertaining to entropy production have been considered in

Energy source	Efficiency %	Principal entropy	Configurational entropy
Gravitational energy	See hydro and wind	See hydro	No significant change
Geothermal energy	50	17, 100, 150 kJ/K	No significant change
Hydro power	90 - 95	3.3 - 723 kJ/K	No significant change
Solar energy	0.4 - 1	No significant change	Possible increase
Wind energy	40	50.3 kJ/K	Possible increase
Biofuels	Depends on application	Increase	Significant increase
Coal	30 - 40	5 MJ/K	Increase
Fission energy	35	6.5 MJ/K	Increase
Fusion energy	N/A	Increase	Decrease

Table 7.1: The table shows a summary of the values estimated in the previous section. They are not completely accurate, and can not be used for any other purpose than a general comparison of the sustainability of the different energy sources based on the definition given by Schrödinger.

this thesis. If we were to draw conclusions on this aspect alone, it is clear from our calculations and discussions that fusion power is the only truly sustainable energy source. Other energy sources, such as hydro power, gravitational energy, and possibly solar power can also be considered quite sustainable, since they do not contribute any significant decrease in complexity. The exception here is if solar panels are built in areas where there otherwise would have been vegetation, or on land suited for agriculture, in which case they can not be considered sustainable. The use of biofuels represents in this definition the least sustainable energy source. It causes an entropy increase both through the energy loss from the conversion of thermal to mechanical energy, in addition to a significant loss in complexity. Fossil sources are in Schrödinger's definition more sustainable than biofuels, since the configurational entropy increase in these sources are inevitable and have already happened naturally. However, both solid and liquid fossil sources are in most cases made to be gas-like before they are burned, contributing to a slight increase in configurational entropy. In addition, they are all thermal energy sources, which causes a significant energy loss through the conversion to mechanical energy, and can therefore not be considered completely sustainable. It can be argued here that the use of natural gas for heating purposes is an exception, since the production of heat is, in this case, the goal. Geothermal energy can also be utilized as a sustainable heat source, but will in electricity generation cause an increase in the principal entropy due to energy loss through conversion.

As we see from table 7.1, the principal entropy production rate per second for a small geothermal and a small hydro power plant are 17 kJ/K and 3.3 kJ/K respectively. When comparing the entropy values of the different sources, it is important to keep in mind what power output the values correspond to. For geothermal and hydro power, these values are 5 MW and 10 MW respectively. We see that per MW produced, the hydro power plant has an even lower entropy production rate compared to geothermal energy than what might seem like from the entropy values alone. This difference is due to the different conversion efficiencies, and it is the reason why a higher efficiency can be associated with a higher degree of sustainability.

The global, annual primary energy consumption is currently about 18 TWyr [6]. In year 2013 Norway produced 134 TWh of electricity. About 129 TWh were produced by hydro power, 1.9 TWh by wind power and 3.3 TWh in gas plants and other thermal power stations. This average total electricity production has been stable around 135 TWh since the new millennium [4]. As we stated in already in this chapter and in chapter 5, hydro power can be considered quite sustainable in Schrödinger's definition, since it has a high conversion efficiency and minimal total entropy contribution. The installation of wind power plants in Norway has not been commercially profitable, but has been subsidized by the government. At the beginning of 2014, Norway had 811 MW installed wind power spread out on 356 turbines in 20 registered wind power plants. These produced 1898 GWh in 2013 [4]. Although Norway has relatively favorable wind conditions, we see that the amount of power produced is only 26.7% of the installed capacity with continuous operation. As stated in chapter 5, wind power can not be considered sustainable in Schrödinger's definition, since it causes an increase in both principal and configurational entropy. This is emphasized by the large area a wind park needs per MW electricity generated compared to most other energy sources. Estimations of such numbers for different energy sources, i.e. unit area needed per unit power generated, would be interesting to compare with our estimations of entropy generation. Such comparative studies are important in order to ensure that the most sustainable options are chosen, and they can be an interesting basis for further studies.

List of Figures

List of Tables

Bibliography

[1] L. P. Csernai, S. F. Spinnangr, S. Velle, *Quantitative Assessment of Increasing Complexity*, Physica A **473** (2017), pp. 363-376.

[2] L. P. Csernai, I. Papp, S. F. Spinnangr, Y. Xie, *Physical Basis of Sustainable Development*, J. Cent. Eur. Green Innov. **4** (2016), pp. 39-50.

[3] R. Ehrlich, *Renewable Energy : a first course*, CRC Press Taylor & Francis Group LLC, (2013).

[4] Olje- og Energidepartementet, *FAKTA 2015 Energi- og Vannressurser i Norge*, (2015).
https://www.regjeringen.no/contentassets/fd89d9e2c39a4ac2b9c9a95bf156089a/1108774830_897155_fakta_energi-vannressurser_2015_nett.pdf (checked 05/31/17)

[5] H. Motz, *The Physics of Laser Fusion*, Academic Press Inc. (London) Ltd., (1979).

[6] J. Ongena, Y. Ogawa, *Nuclear fusion: Status report and future prospects*, Energy Policy **96** (2016), pp. 770-778.

[7] C. McCombie, M. Jefferson, *Renewable and nuclear electricity: Comparison of environmental impacts*, Energy Policy **96** (2016), pp. 758-769.

[8] N. Nakicenovic, L. Gomez-Echeverri, T. B. Johansson, A. Patwardhan, ed., *Global Energy Assessment: Toward a Sustainable Future*, Cambridge: Cambridge University Press, (2012).

[9] J. Freidberg, *Plasma Physics and Fusion Energy*, Cambridge University Press, New York, (2007).

[10] The World Commission on Environment and Development, *Report of the World Commission on Environment and Development: Our Common Future*, (1987).
http://www.un-documents.net/our-common-future.pdf (checked 05/31/17)

[11] E. Schrödinger, *What is Life? The Physical Aspects of the Living Cell*, University Press, Cambridge, (1944).

[12] D. V. Schroeder, *An Introduction to Thermal Physics*, Addison Wesley Longman, (2000).

[13] C. F. Chyba, G. D. McDonald, *The Origin of Life in the Solar System: Current Issues*, Annu Rev Earth Planet Sci **23** (1995), pp. 215-249.

[14] K. H. Norwich, *Boltzmann-Shannon entropy and the double-slit experiment*, Physica A **462** (2016), pp.141-149.

[15] L. Boltzmann, *Further Studies on the Thermal Equilibrium of Gas Molecules*. In: *The Kinetic Theory of Gases, An Anthology of Classic Papers with Historical Commentary*, S. G. Brush, ed., Imperial College Press, (2003), pp. 262-349.

[16] C. E. Shannon, *A Mathematical Theory of Communication*, Bell Syst. Tech. J. **27** (1948), pp. 379-423.

[17] L. Brillouin, *The Negentropy Principle of Information*, Journal of Applied Physics **24** (1953), pp. 1152-1163.

[18] L. P. Csernai, *Introduction to Relativistic Heavy Ion Collisions*, Wiley, (1994).

[19] L. Pénzes, L. P. Csernai, Zeitschrift für Alternsforschung, **35** (1980), pp. 285-296.

[20] Z. Shengjun, W. Huaixin, G. Tao, *Performance comparison and parametric optimization of subcritical Organic Rancine Cycle (ORC) and transcritical power cycle system for low-temperature geothermal power generation*, Applied Energy **88** (2011), pp. 2740-2754.

[21] Z. Wang, Y. Li, K. Wang, Z. Huang, *Environment-adjusted operational performance evaluation of solar photovoltaic power plants: A three stage efficiency analysis*, Renewable and Sustainable Energy Reviews **76** (2017), pp. 1153-1162.

[22] S. Suman, M. K. Khan, M. Pathak, *Performance enhancement of solar collectors - A review*, Renewable and Sustainable Energy Reviews **49** (2015), pp. 192-210.

[23] V. Smil, *Energy Transitions; History, Requirements, Prospects*, Praeger, (2010).

[24] L. P. Csernai, *Detonation on a timelike front for relativistic systems*, Zh. Eksp. Teor. Fiz. **92** (1987), pp. 379-386.

[25] L. P. Csernai, D. D. Strottman, *Volume ignition via time-like detonation in pellet fusion*, Laser and Particle Beams, **33** (2015), pp. 279-282.

[26] D. Elliott, *Tidal Power - Moving Ahead*. In: *Energy Research Developments : Tidal Energy, Energy Efficiency and Solar Energy*, K. F. Johnson, T. R. Veliotti, ed., Nova Science Publishers, Inc. (2010), pp. 95-105.

[27] V. de Laleu, *La Rance Tidal Power Plant : 40-year operation feedback - Lessons learnt*, presented on BHA Annual Conference, Liverpool, England, (2009). http://www.british-hydro.org/downloads/La%20Rance-BHA-Oct%202009.pdf (checked 05/09/17)

[28] Y. Semchenkov, Y. Styrin, *Advancing of VVER Reactor Core*, presented in Varna, Bulgaria, 9-11 June (2010). http://www.bulatom-bg.org/files/conferences/dokladi2010/Section%202/Report_Styrin.pdf (checked 05/10/17)

[29] R. Betti, O. A. Hurricane, *Inertial-confinement fusion with lasers*, Nature Physics **12** (2016), pp. 435-448.

[30] J. D. Lawson, *Some Criteria for a Power Producing Thermonuclear Reactor*, Proc. Phys. Soc. B **70** (1957), pp. 6-10.

[31] E. M. Henley, A. Garcia, *Subatomic Physics*, 3. edition, World Scientific Publishing Co. Pte. Ltd. (2007).

[32] W. T. Sullivan III, J. A. Baross, ed., *Planets and Life : The Emerging Science of Astrobiology*, Cambridge University Press, (2007).

[33] R. Betti, P. Y. Chang, B. K. Spears, K. S. Anderson, J. Edwards, M. Fatenejad, J. D. Lindl, R. L. McCrory, R. Nora, D. Shvarts, *Thermonuclear ignition in inertial confinement fusion and comparison with magnetic confinement*, Phys. Plasmas **17** (2010) 058102.

[34] S. F. Spinnangr, I. Papp, L. P. Csernai, *Radiation dominated implosion*, arXiv:1611.04764

[35] E. I. Moses, *Ignition on the National Ignition Facility: a path towards inertial confinement fusion energy*, Nucl. Fusion **49** (2009) 104022.

[36] P. Breeze, *Power Generation Technologies*, Newnes, (2005).

[37] U. Eberle, B. Müller, R. von Helmholt, *Fuel cell electric vehicles and hydrogen infrastructure: status 2012*, Energy Environ. Sci. **5** (2012) 8780.

CHAPTER 8

Attachment

The following pages are the article *Quantitative assessment of increasing complexity* that was published in Physica A in January 2017. In it the method described in chapter 4 is developed and used to estimate the entropy of complex materials. As mentioned earlier, the calculations and estimates done for DNA and more complex structures that are shown later in the article (sections 5-9) is not my work. They have been done by my supervisor Laszlo Csernai and his PhD student at the time, Sindre Velle. The novel science in our publication is how we show that the kinetic and configurational entropy can be evaluated on the same level. This is what is included in chapter 4 of this thesis.

Physica A 473 (2017) 363–376

Contents lists available at ScienceDirect

Physica A

journal homepage: www.elsevier.com/locate/physa

Quantitative assessment of increasing complexity

L.P. Csernai *, S.F. Spinnangr, S. Velle

Institute of Physics and Technology, University of Bergen, Allegaten 55, 5007 Bergen, Norway

HIGHLIGHTS

- Evaluation of complexity quantitatively for different systems via the entropy of unit amount of materials.
- Unifying definitions of physical phase space entropy and Shannon entropy.
- Demonstrating quantitatively the decreasing entropy of more complex systems.

ARTICLE INFO

Article history:
Received 8 September 2016
Received in revised form 12 December 2016
Available online 4 January 2017

Keywords:
Entropy
Complexity
Development
Sustainability

ABSTRACT

We study the build up of complexity on the example of 1 kg matter in different forms. We start with the simplest example of ideal gases, and then continue with more complex chemical, biological, life, social and technical structures. We assess the complexity of these systems quantitatively, based on their entropy. We present a method to attribute the same entropy to known physical systems and to complex organic molecules, up to a DNA molecule. The important steps in this program and the basic obstacles are discussed.

1. Introduction

The problem of development is longstanding in humanity. It became quantitative with the development of statistical physics and quantum physics. The first theoretical step was done by Boltzmann, who laid down the basis of microscopic quantitative treatment of entropy both for equilibrated and out of equilibrium systems. In the H-theorem he showed that closed systems in equilibrium maximize their entropy, and all microscopic interactions drive the system towards this equilibrium. This macro state is the most probable one the system can reach.

Consequently, a less probable, non-equilibrium state can be formed only if the system is not closed and can exchange entropy with the surrounding, so that its own entropy decreases. Under stationary conditions, constant pressure and temperature, spontaneous chemical reactions do not lead to more complex systems.

These ideas were discussed already by E. Schrödinger in 1943, in his book: "What is life?" [1]. He described that life forms are highly complex systems of a high level of "order", that can develop from disordered systems, or more probably from ordered systems of a somewhat lower level of order. Our ultimate aim is to show at what cost sustainable development is possible, what the direction of sustainable development is, and which processes are working towards such development. We aim to quantify the LEVEL and the RATE of the development quantitatively.

Schrödinger described the problem and the concepts in a genius way, but he could not give quantitative information at that time. We know much more about biological structures and life forms today, so it is possible to discuss these problems quantitatively.

* Corresponding author.
E-mail address: csernai@ift.uib.no (L.P. Csernai).

http://dx.doi.org/10.1016/j.physa.2016.12.091
0378-4371/

Table 1
Thermodynamical parameters of 1 kg material in different forms approximated as ideal gases, depending on their mass numbers, A_P, different mol-numbers of particles, N_P, and this number is decreasing with increasing A_P. The specific entropy of the composite particles is indicated by the dimensionless σ_P ($\hbar$, c, $k_B = 1$). The total entropy of the material at the used $T = 300$ K and $p = 1$ bar, is also decreasing with increasing complexity, i.e. increasing A_P. (For H_2O^* the temperature is taken to be $T = 100\ ^\circ C = 373.15$ K.)

Material	A_P	N_P (mol/kg)	σ_P	$S_{1\ kg}$ (J/K)
H_2	2	496.046	14.146	58344.0
He	4	248.023	15.186	31316.1
H_2O	18	55.116	17.442	7993.0
H_2O^*	18	55.116	17.988	8243.0
Rn	222	4.469	21.211	788.1
WF_6	298	3.329	21.652	599.3
UF_6	352	2.818	21.902	513.2
C60	720	1.378	22.975	263.2

In this work we introduce the method to calculate the entropy of a well defined amount of matter, irrespective of what form of matter we are discussing. This is because the development on the Earth happens with a constant amount of matter, but the forms of matter may change due to nuclear, chemical, biological, technological, intellectual and societal reactions and changes. Thus, we introduce a unit of **1 kg** for our discussion. (Although, for intellectual and societal changes and structures this choice of unit is too extreme in this moment.) The human intellect is the limit where the material form, the nervous system, and the intellectual information content are at the boundary of our knowledge. At this time this program can be performed up to simple structures of actions and simple vegetative nervous systems. For transparency and the illustration of the program we start from the simplest (and highest entropy) systems. We intend to provide a simple and sometimes even simplified presentation of the entropy calculations and the corresponding degrees of freedom of materials.

The second important new aspect we introduce, is to achieve the possibility of comparing different forms of matter with a uniform definition of entropy. In the present literature, in mathematics, information theory, linguistics, etc. many definitions of entropy exist. The most widely known, after the material entropy in statistical physics, is the "Shannon entropy" [2]. We remind the reader that this definition was already used by Boltzmann in the H-theorem for non-equilibrium systems, and this makes it possible to attribute the same physical dimension to both entropies.

A third aspect we have to utilize is the quantization of the phase space entropy by the volume of the phase-space cell. This is an important step in unifying the entropy evaluation and it is not obvious how to perform this for highly complex systems.

The last step is to select the physically realized system configuration(s) from all possible ones with the same degree of complexity and degrees of freedom. In highly complex systems this step is also nontrivial, and for societal or intellectual systems it is even debatable which systems are realized or realizable.

We introduce this system in a series of examples, from the most simple elementary ones up to the most complex ones, which can still be discussed on a quantitative basis. These last examples are from biology, but our aim is not to contribute to quantitative biology, but rather to demonstrate our procedure, how to quantitatively assess the sustainable development following Schrödinger's original ideas.

2. Elementary entropy evaluations for unit amount of matter

In this section we introduce the first steps of our program, with the basic units and definitions using the most simple, generally known systems. For those who are well familiar with statistical physics the sections up to Section 4 or 5 can be skimmed through. Here the importance of quantization and the unified treatment of Gibbs and Shannon entropy are essential.

We can start with the example of more and more complex chemical structures. For example with dilute gases, approximated first as ideal gases.

We take a series of gases, H_2, He, H_2O, Rn, WF_6, UF_6 and C_{60}, with increasing molecular weight or "Particle mass Number", A_P. We take 1 kg of material, so the number of particles, N_P, in this amount of matter will decrease with increasing mass number, A_P. We choose that the gas is at standard atmospheric pressure, i.e. at $P = 1$ atm, and $T = 300$ K temperature.

Using the ideal gas approximation

$$S_{1\mathrm{kg}} = N_P\, k_B \left[\frac{5}{2} + \ln\left(\frac{(2\pi m_P c^2 k_B T)^{3/2}}{n_P (2\pi\hbar c)^3}\right)\right], \tag{1}$$

where k_B is Boltzmann constant ($k_B = 1.38064852 \cdot 10^{-23}$ J/K), m_P is the particle mass, (we take it as $m_P = A_P m_{Nucl.}$ in terms of the nucleon mass, $m_{Nucl.}$) and n_P is the particle density ($n_P = Av/(V_{I.G.})$ in terms of the Avogadro number, Av. The molar volume of an ideal gas is, $V_{I.G.}$ at STP, standard pressure and standard temperature of $T = 273.15$ K). The moderately increasing dimensionless specific entropy per particle, $\sigma_P = S/(k_B N_P)$, is also shown. See Table 1. In the table all values

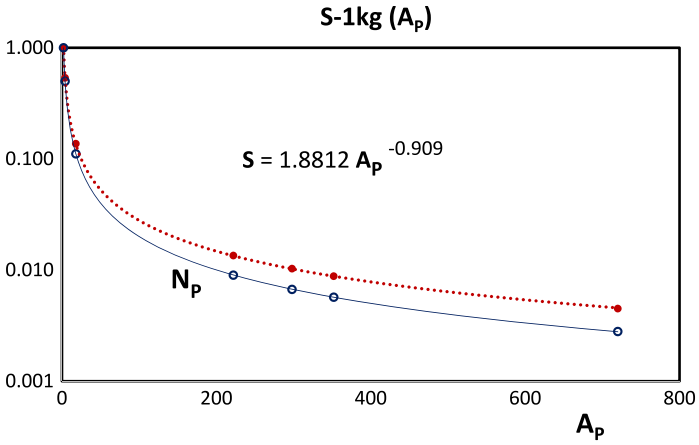

Fig. 1. (Colour online) The mass number, A_P, dependence of the relative entropy of 1 kg material, S, compared to the number of these particles, N_P. The relative entropy, S, as well as the particle number, N_P, of 1 kg H_2 is taken to be unity for the comparison. The entropy decreases slower than the decrease of the particle number. This means that the entropy per particle is increasing.

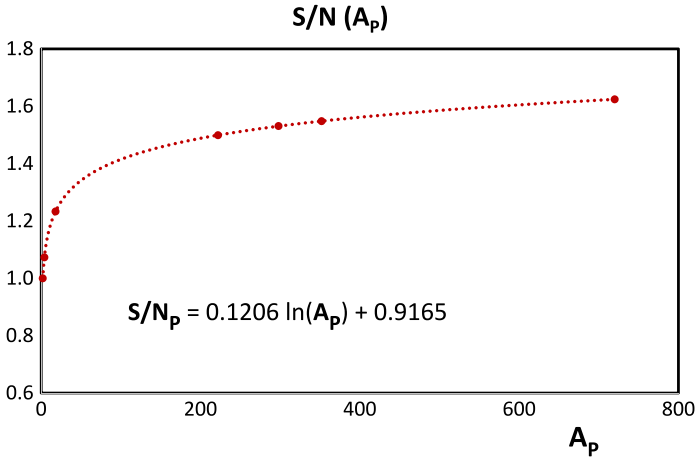

Fig. 2. (Colour online) The change of the relative ratio of entropy versus particle number, S/N_P as a function of the mass number of a given particle species, A_P. For this comparison the S/N_P for H_2 is taken to be unity.

were calculated in the ideal gas approximation and for $T = 300$ K, except the water, H_2O, which is at boiling temperature, $T = 373.15$ K.

Noble gases, He, Rn, and also small molecules, can be well approximated as ideal gases, their vibrational degree of freedom carries negligible energy. Under standard conditions the heaviest couple of materials are not gases and their interactions and internal degrees of freedom should also be taken into account. Thus, for water vapour and for the heavy gases the ideal gas approximation underestimates the entropy of the material.

Nevertheless, even for ideal gases the entropy is not behaving the same way as the particle number. This can be seen well in Fig. 1. Let us take the values of N_P and $S_P(1\text{ kg})$ for H_2 as standard unity, and see how N_P and $S_P(1\text{ kg})$ change with increasing A_P. While N_P decreases according to the $N_P A_P = \text{const.}$ constraint (and therefore $N_P \propto A_P^{-1}$), the entropy, $S_P(1\text{ kg})$, decreases less due to the additional contribution of the log term in the entropy expression $\propto \ln(m_P/n_P)$. Consequently the entropy decreases as $S \propto A_P^{-0.9}$.

This change is shown if Fig. 2, where again the ratio $\sigma_P = S/(k_B N_P)$ for H_2 is taken to be unity. The increasing relative entropy exceeds $S/(k_B N_P) = 1.6$ for C_{60} but it has a saturating tendency. In this ideal gas approximation the ratio is not expected to exceed two.

For larger, more complex molecules the number of degrees of freedom increases, and specific molecular configuration has less entropy than the completely random ideal gas.

Interacting materials can form other liquid or solid phases, which have more constraints, compared to the increasing number of degrees of freedom. This decreases the entropy of a given liquid or solid further. We will illustrate this on the example of water.

As in liquids there is still considerable room for random configurations where entropy is decreasing less than that of the solids, where the level of "order" [1] is higher.

Schrödinger's considerations were extended to lifeforms of matter [1], and similar comparative studies were used for comparing the change of the entropy content of different species during their lifespan [3], as well as the rate of change of the entropy during the life of different species. The initial development phase leads to a considerable decrease of the entropy of

the matter incorporated into the living species (build up of neg-entropy), then the entropy is increasing again in the second stage of the life of the species. The rate of these changes is connected to the energy exchange with the environment (or metabolism) and this then determines the lifespan of a species.

Interestingly Schrödinger discusses two ways on how to achieve a high level of order, (i.e. smaller entropy). High level of order can be built up from dis-ordered materials as well as from an already ordered material with achieving a higher level of order. This second way is obviously easier and preferable.

Interestingly the same fundamental ideas can be extended to the sustainable development of the Earth, and this has also been done for a while, using the principles of statistical physics [4]. The consequences of these more fundamental and more quantitative considerations are interesting. The popular folklore considers some selected energetic processes as sustainable, while others are not. Recently some energy resources are declared "renewable" others are not. In this respect the use of "bio-fuels" is quite problematic, because if we burn or destroy highly complex, biological materials, this may lead to decreasing "order" in Schrödinger's sense, which is not contributing to sustainable development. The same issue may arise if photovoltaic production sites occupy large agricultural territories, which is not taken into consideration.

Therefore our aim is to demonstrate the connection between sustainable development, energy and entropy exchange in a quantitative way, as far as possible.

Furthermore, we want to extend these considerations beyond different life-forms of matter, to technical and social development. In this last point, quantitative energetic and entropy aspects are probably beyond our present knowledge, but one can still estimate which direction of changes certain social actions can or will cause.

3. Network or topological entropy

We can continue the previous simplified study by considering different hypothetical ideal gases constructed from nucleons like H_1, H_2, H_3, H_4. If we consider these as different ideal gases without taking into account the type of binding, then we end up with the result in the previous section. Let us neglect the physical features of a binding, such as its energy or extra degrees of motion, and only consider the possible topologies of the binding. If we take the molecule H_2, then we have a link between two nucleons. For this molecule we can only insert a link one way to make a cluster, so the existence of the link does not contribute to extra energy or entropy (because we neglected the small rotational or vibrational energies).

In both cases (H_1 and H_2) there is only one configuration for the molecule, i.e. $i = 1$ and $p_1 = 1$, and the sum of all allowed configuration states is, N, is $N = 1$. Thus, the topological Shannon entropy of these molecules is

$$H(X) = -p_1 \ln p_1 = 0. \tag{2}$$

If N would be $N > 1$, then the most random configuration would be $p_i = 1/N$ for each i and so for this configuration the Shannon entropy is

$$H(X) = -\sum_{i=1}^{N} p_i \ln p_i = -N \frac{1}{N} \ln \frac{1}{N} = \ln N = H_{\max}. \tag{3}$$

Let us now consider a (hypothetical) H_3-molecule. This can be formed by inserting (2) links or (3) links! Thus, we can have two characteristic structures for 3 nucleons. Two links, (2), can be inserted 3 ways: 12 & 23 or 13 & 23 or 13 & 12 for identical but distinguishable nucleons. Three links, (3), can be inserted only one way, 123, for identical particles. The two link configurations can be obtained from the three link ones by cutting one link and this can be done in three ways. This is altogether 4 configurations, with (3) being $i = 1$ and (2) being $i = 2$, then $p_1 = 1/4$ and $p_2 = 3/4$ (see Fig. 3). The Shannon entropy of a system X with all possible configurations of the H_3 molecule is then

$$H(X) = -\left[\frac{1}{4} \ln \frac{1}{4} + \frac{3}{4} \ln \frac{3}{4}\right] = 0.5623. \tag{4}$$

If we consider a (hypothetical) H_4-molecule, then the maximum number of connections is 6 and the minimum number (keeping still a bound cluster) is 3. A molecule with 5 bounds can be obtained by cutting one of the 6 bounds, and this can be done 6 ways. A molecule with 4 bounds can be obtained by cutting one more bound, as the lines are indistinguishable we do not take the order of which we remove the lines into account. This can then be done in $6 * 5/2$, so altogether this gives 15 configurations, but these will have two different topological configurations:

(4A) 1 way with each node having 2 links, i.e. in tot. $N_{(4A)} = 3 * 1$ ways and
(4B) 4 ways with nodes having 1, 2, 2 & 3 links, i.e. in tot. $N_{(4B)} = 3 * 4$ ways.

Then with a further cut (4A) leads to a linear chain with 3 links (3A) which can be obtained 4 ways, i.e. in tot. $3 * 1 * 4/3$ ways. The (4B) configuration leads to the (3A) chain in 2 ways by cutting one of the links at the 3-link node, in tot. $3 * 4 * 2/3$ ways. Thus the (3A) configuration can be reached in total $N_{(3A)} = 3 * 4 * 3/3$ ways.
There is a further 3 link configuration which can be generated from (4B) by cutting the link between the two 2-link nodes, this can only be done one way, i.e. $N_{(3B)} = 3 * 4 * 1/3$ ways in total (see Fig. 4).

Thus the (6) and (5) link structures have only one type of topological configuration, although with different topological formation probabilities, the (3) and (4) link configurations have two types of topological configurations, A and B, and

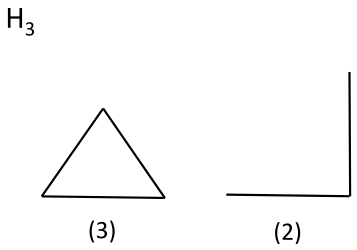

Fig. 3. The topological configurations of hypothetical H_3 molecules, according to the number of links in a given configuration, (3) or (2). These configurations can be formed in $N_i = 1, 3$ ways respectively.

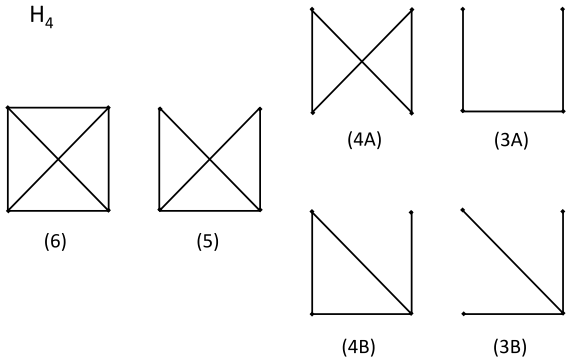

Fig. 4. The topological configurations of hypothetical H_4 molecules, according to the number of links in a given configuration, (6), (5), (4A), (4B), (3A), (3B). These configurations can be formed in $N_i = 1, 6, 3, 12, 12, 4$ ways respectively.

these have different topological formation probabilities. The sum of all configurations is $N = \sum_i N_i = 38$ and so, $p_i = N_i/N = 0.0263, 0.1579, 0.0789, 0.3158, 0.3158, 0.1053$.

If all these configurations are realized, with the above probabilities then the Shannon entropy of the system is

$$H(X) = -\sum_{i=1}^{N} p_i \ln p_i = -\sum_{i=1}^{6} \frac{N_i}{N} \ln \frac{N_i}{N} = 1.5526. \tag{5}$$

This entropy is a sum of all six possible configurations. The entropy of these six subsets is additive so we can also calculate the entropy of a given configuration or of a subset of configurations. Thus for the configuration $X = (4A)$, we obtain

$$H(4A) = 0.3662. \tag{6}$$

Thus the connection or network topology should also be taken into account. We can consider this on the hypothetical example of H_1, H_2, H_3, H_4 gases, with and without taking into account the topological entropy.

In real physical situations, not all (hypothetical) configurations are realized. Furthermore, the links also have energies, so the experimental probabilities are not exactly the same as the topological estimates. Nevertheless, this topological example is able to give guidance on how to take topological (or network) structures into account in entropy estimates.

In the case of usual (Shannon) entropy estimates, the normalization is not the same as the physical one, but it is perfectly sufficient for comparative studies of these types of structural entropies.

Now the question arises, how do we add this configuration entropy to the expression in Eq. (1)? For this purpose we convert both definitions into dimensionless form. The configuration entropy, i.e. the Shannon entropy is already in dimensionless form. Boltzmann's original definition for any (non-equilibrium) system has also the same structure. The definition for one particle

$$H(X) = \sigma_P = \frac{S}{k_B N_P} = -\sum_{i=1}^{N} p_i \ln p_i, \tag{7}$$

may define both the sum for the probabilities of all configurations, p_i^c, or the sum for all probabilities to be in a phase space volume element, p_i^p, of size $(2\pi\hbar)^3$. This in this latter case is

$$p_i^p = (2\pi\hbar)^3 f(x, p), \tag{8}$$

where $f(x, p)$ is the phase space distribution function normalized for one particle. In this latter case σ_P is the dimensionless specific entropy for one particle (or molecule), which can be obtained from the physical entropy S as given by Eq. (7).

For a relativistic gas, the entropy density, using Boltzmann's definition for any equilibrium or non-equilibrium phase space distribution, $f(x, p)$, is [5]

$$s(x) = -\int \frac{d^3p}{p^0} p^\mu u_\mu f(x,p) \left[\ln\left((2\pi\hbar)^3 f(x,p)\right) - 1\right], \tag{9}$$

where $p^\mu u_\mu$ is the frame invariant relativistic expression for the local energy density. The last term, -1, ensures the appropriate entropy constant for joining smoothly the low temperature quantum statistical limit in case of Boltzmann statistics.[1]

If we reach an equilibrium, we have a stationary solution of the Boltzmann Transport Equation, e.g. the Jüttner distribution, $f(x, p)$, and the entropy becomes

$$s(x) = -\int d^3p\, f(x,p) \left[\frac{\mu}{T} - \frac{\varepsilon}{T} - 1\right]. \tag{10}$$

Here μ is the chemical potential, T is the temperature and ε is the specific energy, the energy for one particle. Notice that in the relativistic theory both μ and ε includes the rest mass of the particle, but in the entropy expression these terms cancel each other. In the non-relativistic limit for the Boltzmann distribution this leads to the entropy expression of Eq. (1).

If the phase space distribution is normalized to $n_P(x)$, i.e.

$$n_P(x) = \int d^3p\, f(x,p), \tag{11}$$

then the entropy for one particle can be obtained for the Boltzmann statistics as

$$\sigma_P^{ph.s.} = \frac{s}{k_B\, n_P} = -\sum_{i\epsilon\ ph.s.} p_i^p [\ln p_i^p - 1] \tag{12}$$

where $p_i^p = (2\pi\hbar)^3 f(x,p)$, the probability to be in a phase space cell, i, should be calculated for one particle, i.e.

$$\int d^3x\, n_P(x) = 1. \tag{13}$$

Still the entropy, the distribution function and p_i^p depend on the particle density, n_P.

Thus in conclusion the single particle entropies should be additive in a configuration

$$\sigma_P = \sigma_P^{conf.} + \sigma_P^{ph.s.} = -\sum_{i\epsilon\ conf.} p_i^c \ln p_i^c - \sum_{i\epsilon\ ph.s.} p_i^p [\ln p_i^p - 1], \tag{14}$$

where p_i^c, is the probability to have a configuration state, i. In conclusion the increase of the degrees of freedom due to the different configurations leads to an increase in the single particle entropy. This increase is very small if the number of possible configurations, $N = \sum_i N_i$ is large, but the number of a realized configurations, N_i, is much smaller, $N_i \ll N$.

In the above discussed estimate we only considered differences in topological configuration among identical particles. In real situations the complexity may increase due to: direction dependence of the links, different constituents, different (energetic) weights of the links, dynamical freedom of the length or angle of the link, etc.

In Table 2 the hypothetical ideal gas particles, H_1 and H_2, have no option for different configurations. For H_3, the specific entropy, σ_P, increased by a relatively small amount of 0.347 and 0.216 for the topological configurations $H_3^{(3)}$ and $H_3^{(2)}$ respectively. The entropy of the different H_4 configurations is increased by small values of configuration entropy between 0.096 and 0.364. The increase in configuration entropy is very small for configurations with small probability, p_i, which may occur for complex systems with a large number of possible configurations where only a few are realized in a realized sample of configurations.

The configuration entropy may be much larger for more involved structures, where the number of configurations are comparable or may even exceed the number of particles. Also, an important question to ask is how many of these configurations can be realized, and how many are actually present in a given sample we discuss.

4. Entropy of phases of physical systems

Physical systems may have a variety of configurations, different (i.e. nonidentical) constituents, and different physical degrees of freedom, such as vibration, rotation, etc., in addition to the phase space occupancy. Because of this, their entropy may well exceed the entropy based on the ideal gas approximation. e.g. 1 kg ideal gas with mass number 18 (H_2O) has an entropy of $S_{1\ kg} = 8243.0$ J/K, at the boiling point, while the physical value is about 10 495 J/K. This can be explained by the different types of constituents, H and O, the configuration and other dynamical degrees of freedom and types of interactions (see Fig. 5).

[1] For Fermi–Dirac or Bose–Einstein distributions the additional term, -1, does not appear, but at the same time the calculation of the probabilities of the phase space cell occupations is more involved.

Table 2
Entropies of a single composite particle and of 1 kg material in different topological configurations for hypothetical H_1, H_2, H_3 and H_4, molecules approximated as ideal gases, depending on the mass numbers, A_P, of the nucleons in the molecule and the configuration where it is indicated. 1 kg material contains different mol-numbers of particles, N_P, and this number is decreasing with increasing A_P. The specific entropy of the composite particles is indicated by the dimensionless ($\hbar$, c, $k_B = 1$) σ_P. The total entropy of the 1 kg material at STP is also decreasing with increasing complexity, i.e. increasing A_P.

Material	A_P	N_P (mol)	σ_P	$S_{1\ \mathrm{kg}}$(J/K)
H_1	1	992.092	13.106	108111.7
H_2	2	496.046	14.146	58344.0
H_3	3	330.697	14.754	40568.3
$H_3^{(3)}$	3	330.697	15.101	41521.2
$H_3^{(2)}$	3	330.697	14.970	41161.6
H_4	4	248.023	15.186	31316.1
$H_4^{(6)}$	4	248.023	15.282	31513.5
$H_4^{(5)}$	4	248.023	15.477	31917.1
$H_4^{(4A)}$	4	248.023	15.386	31729.5
$H_4^{(4B)}$	4	248.023	15.550	32066.8
$H_4^{(3A)}$	4	248.023	15.550	32066.8
$H_4^{(3B)}$	4	248.023	15.423	31804.8

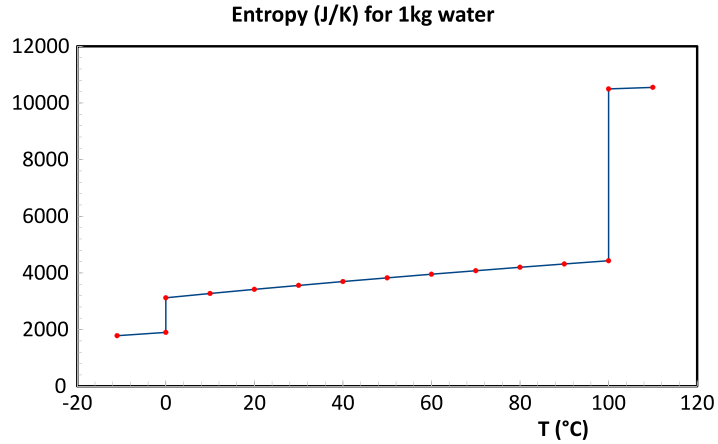

Fig. 5. (Colour online) Entropy of 1 kg of water at different temperatures, with all three phases, ice, water and vapour, with two phase transitions at 0 and 100 °C. The reference point is taken at $T = 100$ °C liquid water, with entropy of $S_{1\ \mathrm{kg}} = 4430.01$ J/K, where the phase transition to vapour with a latent heat of $\Delta S = 6065.55$ J/K, leads to a vapour entropy of $S_{1\ \mathrm{kg}} = 10495.56$ J/K. Using the water heat capacities we reach the phase transition between water and ice with water entropy of $S_{1\ \mathrm{kg}} = 3122.92$ J/K and ice entropy of $S_{1\ \mathrm{kg}} = 1900.15$ J/K.

If we add the topological configuration entropy, $\sigma_P^{conf.}$, to the ideal gas estimate of the H_2O^* molecule (at $T = 100$ °C), we get a larger value. Here we have two possibilities, the two Hydrogen atoms can be identical (or not). In these two cases we have 3 (or 4) possible topological configurations, see Fig. 6. The specific topological configuration entropies, $\sigma_P^{conf.}$, can be calculated as in Section 3. Here we assume equal probability for each topological configuration. There are four possible cases: either all possible configurations are realized or only a single one, and either the H atoms are identical ($N = 4$ possible cases) or not ($N = 3$ possible cases). Then, the entropy can be calculated as:

$$\sigma_P^{conf.} = -\sum_{i=1}^{N} p_i \ln p_i = \ln N \quad \text{or} \quad \sigma_P^{conf.} = -p_i \ln p_i, \tag{15}$$

for all configurations or a single one respectively. These additive topological configuration entropies are given in Table 3, together with the total entropy values where the entropy from the phase space occupation, $\sigma_P^{ph.s.} = 17.988$ and for the topological configuration are added up.

If all three (or four) configurations would be realized with the same probability then we get a larger final specific entropy, $\sigma_P = \sigma_P^{conf.} + \sigma_P^{ph.s.} = 19.087(19.374)$ and the corresponding entropy for 1 kg material will become $S_{1\ \mathrm{kg}} = 8746.6\ (8878.3)$ J/K. If only one configuration is realized from the three (or four) possible ones, then the final entropies are smaller. For the specific entropy $\sigma_P = 18.354\ (18.335)$ while for 1 kg of material $S_{1\ \mathrm{kg}} = 8410.9\ (8402.1)$ J/K. These last smaller values indicate that the larger information content (i.e. that only one state is realizable from the possible ones) decreases the entropy of the given material.

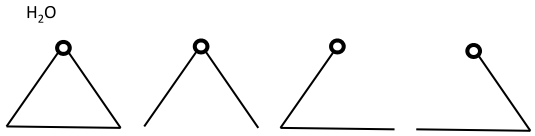

Fig. 6. The topological configurations of a H_2O molecule. The circle indicates the Oxygen atom. If the two H atoms are identical then the last two configurations are identical also.

Table 3
Topological configuration entropy and total entropy of 100 °C water vapour. The realistic physical case is in the last column.

	All 4	All 3	One of 4	One of 3
$\sigma_P^{conf.}$	1.386	1.099	0.347	**0.366**
σ_P	19.374	19.087	18.335	**18.354**
$S_{1\ \mathrm{kg}}^{conf.}$ (J/K)	635.1	503.63	159.02	**167.7**
$S_{1\ \mathrm{kg}}$ (J/K)	8878.3	8746.8	8402.2	**8410.9**

We see that the estimate that includes the addition of topological entropy moved the estimated entropy of the system closer to the experimentally observed value. Obviously, we did not reach the experimental value as several other degrees of freedom (angles, lengths, etc.) were not taken into account, nor the energetic configuration of the water molecule in the vapour.

The exact absolute values of ice are less well known, because the ice has several different configuration structures and it is difficult to make measurements down to 0 K temperatures. The theoretical calculation of complex energetic structures is difficult and the theoretical calculations of structural changes of a phase transition is even more so.

At the phase transitions the heat capacity has a pole, which is again problematic to calculate, so the exact "calculation" of absolute entropies is already difficult for relatively simple molecules with a phase transition.

Nevertheless, we attempt to estimate the absolute entropy values of more complex molecules also, where experimental entropy measurements do not exist. *There are no fundamental reasons to prevent us from estimating the absolute entropies of highly complex molecules.*

For the fundamental determination of absolute entropy values it is important that (i) we quantized the phase space cells with a well defined physical value, and (ii) we connected the entropy to a well defined amount of matter and its energy.

The role of configuration entropy is in principle clear. The 3 atoms of water belong to the above discussed configurations, but the weight of the different probabilities for these configurations are of course different because the connections carry energy, which depends on the "angle" of the two H atoms in the H_2O molecule. Or more precisely, these depend on the characteristic angle of the quantum mechanical wave function of the molecule. In different model calculations this angle varies between 104.52° and 109.5°, and it may also be dependent on the density and temperature of the material.

This feature indicates that the probabilities of the real physical configurations may not be the same as in the oversimplified configuration estimates presented in the previous section. Some configurations can have a highly suppressed probability, or might not be realized at all in nature. E.g. for water the probability of first configuration in Fig. 6, is probably much smaller (based on the wave-function) than in the above topological estimate.

We will see that in more complex structures, there are possible configurations which do not appear in nature at all. To find out which configurations are realized and with what probability, is a much more difficult question than just counting up the number of possible configurations.

The ratio of configuration entropy to kinetic entropy: In Table 1 one we could see that the kinetic entropy increases with increasing particle mass, but this increase is rather slow. Furthermore, this table was calculated with the ideal gas approximation i.e. like the water vapour phase of water. If we consider liquid water at a lower temperature, e.g. room temperature, the entropy of the system is reduced by about 60%, as shown in Fig. 6. While for water vapour the ratio of kinetic entropy to configuration entropy is roughly 20:1, for liquid water at room temperature it is only about 5:1! With more complex molecules the weight of configuration entropy increases further and it may overcome the kinetic entropy.

5. Entropy of complex molecules

As the example of water indicates, more complex molecular structures decrease the entropy compared to the ideal gas approximation. This is due to the interaction among the atoms of a molecule, as well as the interactions among the molecules in a given amount of material. Both these effects decrease the available phase space (e.g. compared to the ideal gas), and therefore these interactions also decrease the entropy. Especially the momentum space degrees of freedom are reduced as the interactions hinder the possibility of large momentum differences among the atoms of a molecule as well as among the molecules.

Furthermore, the atoms of a complex molecule may take different spatial configurations. This was not considered in the previous topological configuration estimates. The spatial configurations of the molecules depend also on the surroundings,

so that a given molecule may have different configurations with different entropies. Especially in biology, these different configuration possibilities have important physiological roles. In case of molecules, these configurations are determined energetically, and can (in principle) be calculated based on the interaction energies within the molecule and among the molecules. Thus, the quantization of the phase space still enables us to obtain the absolute entropy of a given configuration. At a given temperature, one can also determine which configurations are realized, and with what probability. An example of such calculations is the calculation of protein and other molecule conformations, which is a widespread activity today.

The entropy of such a complex molecule is estimated indirectly via the Helmholtz free energy, F, where with the inverse temperature, $\beta = 1/(k_B T)$ we can calculate

$$\beta F(T, V) = -S + E/(k_B T). \tag{16}$$

The effect of interaction is estimated via the correlation function of the density [6], by considering the atoms as hard spheres.

The same type of approximation is used in Ref. [7], where the possible stable (or energy minimizing) packings were counted, and the Gibbs and Edwards (Boltzmann) entropy values were evaluated as a function of the system size. Obviously the number of possible configurations is much larger this way than in the previous topological estimates, but at the same time the locally energy minimizing configurations are considerably fewer than all configurations.

By counting the disordered 3D sphere packings this way the configuration entropy in the spatial occupation can be estimated. In the context of granular packings, our aim is to compute the number of ways, Ω, in which N spheres can be arranged in a given abstract volume of dimension d. Then the total available abstract volume in dN-dimensional space is ν. We can consider the volume of the basis of attraction of each atom in the molecule, in a distinct energy minimum

$$\nu = \sum_{i=1}^{\Omega} \nu_i, \tag{17}$$

where ν_i is the volume of the ith basin of attraction, Ω is the total number of distinct minima and ν is the accessible volume. Thus,

$$\Omega = \frac{\nu}{\langle \nu \rangle}, \tag{18}$$

where $\langle \nu \rangle$ is the mean basin volume. Then the (Gibbs) entropy can be obtained as

$$S_G = -\sum_{i=1}^{\Omega} p_i \ln p_i - \ln(N!), \tag{19}$$

where $p_i = \nu_i/\nu$. A basic estimate is that the dimensionless entropy is

$$S_G \approx N/2, \tag{20}$$

for molecules of up to $N = 100$ atoms [7]. Then the entropy increases slower. So, we estimate that for very large molecules the specific spatial configuration entropy increases slower, e.g. as $\propto \ln N$.

In case of a given bio-molecule, like the DNA, not all spatial configurations are realized. Consequently the sum in Eq. (19) is reduced to a single configuration or to a few configurations, which results in a specific entropy of the order

$$S_G = -p_i \ln p_i - \ln(N!) \approx \frac{\langle \nu \rangle}{\nu} \ln\left(\frac{\langle \nu \rangle}{\nu}\right), \tag{21}$$

and since $\nu = N \cdot \langle \nu \rangle$

$$\sigma_G \approx \frac{1}{N} \ln(N). \tag{22}$$

Therefore, in the specific entropy per 1 kg or per atomic number, the contribution is of the order of one and decreasing with increasing number of atoms, $N = N_a$, in the molecule.

As in most of the literature, these approaches give an entropy value which serves well for the comparison of different complex molecular configurations. At the same time, an absolute entropy value for a given complex molecule and for a given spatial configuration is not given, although this could in principle be possible.

The physical entropy of a complex molecule can be calculated based on all degrees of freedom in the phase space, and all interactions among the constituent atoms. In real situations, to calculate all possible realized and not realized configurations with their energies, is beyond our possibilities. So many different approaches were constructed based on the interconnected network of the constituents [8]. This way static entropies may characterize the global disorder of network topology. One of the approaches to define network entropy is based on the number of the neighbours of a node. This is a degree-based entropy, meaning it is low when the degree of the nodes is uniform and small. There exists more complex definitions of entropy, which account for the interaction between all possible pairs of nodes. The analysis of the entropy of representative subnetworks has also become possible.

Large molecules can form **polymers**, or even larger macromolecules, which are composed of many repeated subunits. These may have a broad range of properties in the case of both synthetic and natural polymers. In these cases the previous dense packing approach is not applicable.

6. DNA in bacteria

The level of complexity is increased in live structures that can replicate themselves. The basis of this replication is the deoxyribonucleic acid (DNA) molecule, which structure is a double spiral. The DNA stores a code made of four chemical bases: adenine (A), guanine (G), cytosine (C) and thymine (T). The sequence of these bases determines the information available for building and maintaining an organism. DNA bases pair up with each other, A with T and C with G, to form units called base pairs. Each base is also attached to other molecular structures which together, the base and its support, is called a nucleotide. The DNA can replicate, or make copies of itself. Bacteria, as asexual organisms, inherit identical copies of their parent's genes.

The average weight of a DNA base pair (bp) is 650 daltons or 650 AMU (where 1 AMU $= 1.660539040(20) \cdot 10^{-27}$ kg $= 931.4940954(57)$ MeV/c^2.)

One of the smallest live systems is the endosymbiotic[2] bacteria Candidatus Carsonella ruddii (CCr), which has $N = 159\,662$ base pairs. Its genome is built up by a circular chromosome.

The possible number of configurations of this number of **base pair sequences** is 4^N, so the probability of the single existing CCr sequence is $p_i = 4^{-N}$. The corresponding base pair sequence entropy is then

$$\sigma_P^{bp} = H(X) = -p_i \ln p_i = -4^{-N} \ln 4^{-N} = N 4^{-N} \ln 4 = 1.386\, N\, 4^{-N}, \tag{23}$$

thus

$$\ln H(x) = -(1.386N) + \ln N + \ln 1.386 = -221\,291.532 + 11.981 + 0.326 = -221\,279.225 \approx -2.2 \cdot 10^5. \tag{24}$$

Thus, the specific entropy of the CCr DNA molecule on the base pair sequence configuration is

$$\sigma_P^{bp} \approx e^{-221\,279} = 10^{-96\,099}. \tag{25}$$

The DNA of the CCr is 159 662 base-pairs and its weight is $m_{DNA_{CCr}} = 159\,662 \cdot 650$ AMU $= 7.727 \cdot 10^{-18}$ kg. So, the number of CCr DNA molecules in 1 kg is $N_{DNA_{CCr}} = 1/m_{DNA_{CCr}} = 1.294 \cdot 10^{17}$.

The entropy of 1 kg of the DNA molecules based on their b.p. configuration is then

$$S^{bp}_{1\text{ kg-CCr}} = k_B\, N_{DNA_{CCr}}\, \sigma_P^{bp} = 1.786 \cdot 10^{-96\,105}\ \text{J/K}. \tag{26}$$

This DNA in the CCr bacteria builds up circular chromosomes. In the physical phase space the momentum part is largely negligible but the **spatial configuration** is substantial. For an exactly given sequence of length, in this case 159 662 base pairs, the number of possible spatial configurations is large. It builds a circular chromosome, but even if the sequence is fixed, the shape can be different. For cell replication one might need a more straight configuration, and other more compact configurations are also possible although these might be energetically less favourable. Here we cannot estimate energetically all possible configurations and their probability. Instead, we make an overly simplified estimate.

The stretched out DNA could expand a sphere of radius $R = N/2$ with a volume of $V = 4\pi R^3/3 = V = \pi N^3/6 = 8.673 \cdot 10^{30}$. If we position the 1st base-pair to a certain location, the next base pair can be put to ∼25 neighbouring points (if these are not occupied). As the volume is 25 orders of magnitude larger than the number of base-pairs, we can neglect the possibility that a chosen point is already occupied. Thus the estimated number of all connected spatial configurations can be

$$M = 25^N. \tag{27}$$

Here we assumed that the base-pairs can be connected in any angle within a cubic grid.

The number of circular configurations is much smaller. The circle has a circumference of N and the diameter of the circle is $D = N/\pi$. Let us choose a random point on the circle. Next, let us choose the opposite point, which is on a sphere of $4\pi D^2$. These two points give an axis of the circle. The third point should set the plane of the circle, which is on a circle of length $D\pi$. After we have chosen these three points, the circle is fixed and there is no more freedom. So the number of possible circles is

$$M_c = 4\pi D^2 \times D\pi = 4\pi^2 D^3 = 4N^3/\pi. \tag{28}$$

Thus the probability of an arbitrary spatial configuration is $p_i = 1/M$, and the spatial configuration (s.conf.) entropy is

$$\begin{aligned}\sigma_P^{s.conf.} &= H(X) = -\sum_{i=1}^{Mc} p_i \ln p_i = \frac{M_c}{M} \ln M = \frac{4N^3}{\pi 25^N} \ln 25^N = \frac{4N^3}{\pi 25^N} N \ln 25 = \frac{4\,3.219}{\pi} 25^{-N} N^4 \\ &= 4.099 N^4 25^{-N}\end{aligned} \tag{29}$$

[2] Endosymbiont is an organism that lives within the body or cells of another organism.

thus

$$\ln H(X) = 1.411 + 4 * \ln N - N \ln 25 = -513\,902.644 \approx -5.139 \cdot 10^5. \tag{30}$$

Thus, the specific entropy of the CCr DNA molecule on the spatial configuration is

$$\sigma_P^{s.conf.} \approx e^{-513\,903} = 10^{-223\,183}. \tag{31}$$

This is a similarly low specific entropy as the one from the base-pair sequence, Eqs. (23)–(24). The entropies from these two independent degrees of freedom should be added

$$\sigma_P = \sigma_P^{bp} + \sigma_P^{s.conf.}, \tag{32}$$

where actually the larger σ_P^{bp} dominates, so that

$$\sigma_P^{DNA} \approx 10^{-96\,099}. \tag{33}$$

The entropy of the DNA molecules in 1 kg matter is then

$$S^{DNA}_{1\text{ kg-}CCr} = k_B\, N_{DNA_{CCr}}\, \sigma_P^{DNA} = 1.786 \cdot 10^{-96\,105}\text{ J/K}. \tag{34}$$

This is the same as the entropy of the DNA b.p. configuration only, Eq. (26), because the entropy from the spatial configuration is utterly negligible.

If we would count the spatial configuration only that would give a smaller specific entropy value, and the resulting entropy for the DNA molecules would yield a smaller value

$$S^{s.conf.}_{1\text{ kg-}CCr} = k_B\, N_{DNA_{CCr}}\, \sigma_P^{DNA} = 1.786 \cdot 10^{-223\,191}\text{ J/K}. \tag{35}$$

7. Entropy of the CCr bacterium

Without its **environment** the DNA molecule cannot exist. If we want to calculate the entropy of one kg material we have to estimate the other surrounding constituents of in the CCr bacteria, in comparison with the DNA in the cell.

The total weight of a CCr bacterium can be estimated to $m_{CCR} \approx 2.3 \cdot 10^{-17}$ kg, i.e. about three times bigger than the weight of the DNA, so two thirds of this weight is made up of smaller molecules than the DNA. The number of CCr bacteria in 1 kg is $N_P = m_{CCR}^{-1} = 0.4 \cdot 10^{17}$/kg. Two thirds of this matter is approximated to be water, and one third of the weights is given by the DNA molecules.

The number, and thus the entropy, of the DNAs in 1 kg CCr bacteria is then about three times less than estimated in Eq. (49)

$$S^{DNA}_{1\text{ kg-}CCr} = k_B\, N_P\, \sigma_P^{DNA} = 0.595 \cdot 10^{-96\,105}\text{ J/K}. \tag{36}$$

For a first, extremely rough estimate, we can assume that this extra material has about the same entropy as water, $S^{H_2O}_{1\text{ kg}} \approx 4000$ J/K. If we then calculate the entropy of 1 kg CCr bacteria:

$$S^{CCr}_{1\text{ kg}} = \frac{2}{3} S^{H_2O}_{1\text{ kg}} + S^{DNA}_{1\text{ kg}} = 2666\text{ J/K} + 0.595 \cdot 10^{-96\,105}\text{ J/K}. \tag{37}$$

Thus, the contribution of the DNA would be utterly negligible to the total entropy of 1 kg CCr bacteria. The replacement of smaller molecules by water overestimates the entropy unrealistically.

A more realistic estimate is that the DNA leads to the build up of different molecules in the cell. Their number and variation depends on the DNA, but also on the environment (!). Due to the larger number and weight of these other molecules of large variation and complexity, the possible number of variations increases, compared to the possible variations of the DNA structure. At the same time, the number of realized configurations can be an even smaller proportion, due to the additional selection caused by the environmental conditions. In conclusion, we can estimate that the complexity of all the smaller molecules of the cell is larger, and their entropy is smaller, than the one estimated from the complexity of the DNA molecule itself (see Fig. 7).

Based on this reasoning, for unit mass, the entropy of all the smaller molecules may be even smaller than the entropy of the DNA, so the more realistic estimate for the entropy of 1 kg CCr bacteria is

$$S^{CCr}_{1\text{ kg}} = k_B\, N_P\, \sigma_P^{DNA} = 1.0 \cdot 10^{-1\,000\,000}\text{ J/K}. \tag{38}$$

It is still amazing to estimate and see, how extremely small the entropy of the most complex molecules and structures is.

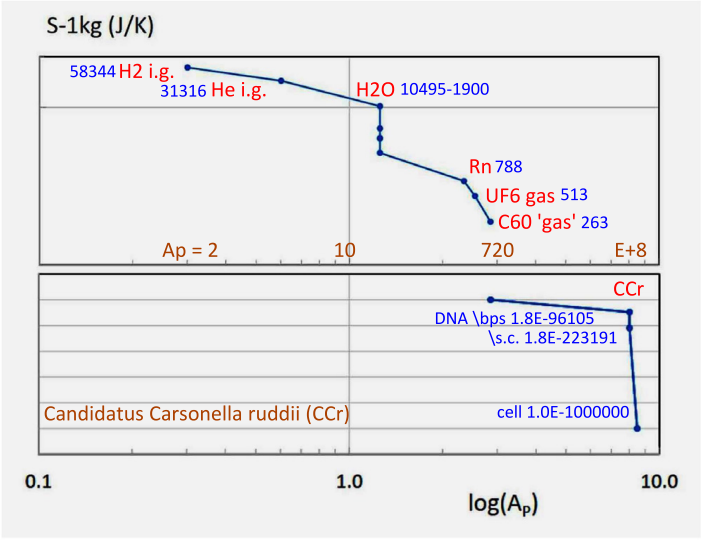

Fig. 7. (Colour online) The entropy of 1 kg material, $S_{1\ \mathrm{kg}}$ in units of (J/K) from light molecules behaving like ideal gases up to the DNA of the simplest bacterium, Candidatus Carsonella ruddii. This last one is based on its base-pair sequence (bps), its spatial configuration (s.c.), and all other different molecules inside the cell. The entropy values are plotted versus the atomic number of the molecules, which is the weight of the molecule in daltons.

8. Entropy of highly complex molecules

The building blocks of DNA are the nucleotides, Thymine, Adenine, Guanine and Cytosine. Each Thymine connects to an Adenine and each Guanine connects to a Cytosine. This is one *allele*. Such a pair is called a nucleotide *base pair*.

The number of DNA base pairs (DNA-bp) in the total human genome (in the 23 chromosomes) is approximately 3.2 billion ($A_P^{DNA\text{-}bp} = 3.234 \cdot 10^9$). Each chromosome is a curled up DNA molecule. In these DNAs there are some 20 000–25 000 genes that contain these base pairs. Genes are sections of the DNA which act as instructions to make molecules, e.g. proteins. Genes with a smaller amount of base pairs (smaller DNA section) will have a higher entropy per mass while a longer DNA section will decrease the entropy.

The human body contains approximately 10 trillion (10^{13}) cells and each of those typical cells contain the genome, i.e. 23 chromosome pairs. There is then approximately $6.4 \cdot 10^{22}$ base pairs in total, but since the genome is the same in each cell, the cell count does not increase the sequential configuration entropy from DNA.

The total amount of all sequences is $N_{all\text{-}sequences} = 4^N$, where N is the number of base pairs,

$$N_{bp} = A_P^{DNA\text{-}bp}.$$

Assuming that all sequences are of equal probability, then for a given sequence, k, the probability is $p_k = 1/4^{N_{bp}}$ and we get

$$H_{\max} = \ln 4^{N_{bp}} = N_{bp} \ln(4) = 4.482 \cdot 10^9 \tag{39}$$

by adding up all these probabilities for $k = 1, \ldots, 4^{N_{bp}}$. This is the Shannon entropy for an ensemble where all possible DNA sequences were realized. If all humans would have the same unique DNA sequence then the Shannon entropy of a human and of the identical species would be

$$\sigma_P^{bp} = H(X) = -p_i \ln p_i = 1/4^{N_{bp}} \cdot \ln 4^{N_{bp}} = N_{bp} \cdot \ln 4/4^{N_{bp}} = 1.386 N_{bp}/4^{N_{bp}} \tag{40}$$

and thus for a single sequence without any variation in the species:

$$\ln H(X) = \ln(4.483 \cdot 10^9) - N_{bp} \ln 4 = -4.483 \cdot 10^9. \tag{41}$$

Single Nucleotide Polymorphisms

Every human is genetically different, and one of the most common genetic variations is called Single Nucleotide Polymorphisms (SNP). An SNP could be the replacement of Cytosine with Adenine for example. The two possible variations are two *alleles* for this base position.

Let us now estimate the number of different sequences in the whole human genome (i.e. in the total of 23 chromosomes or 23 DNAs). One person has only one DNA sequence in each of his or her cells (except mutations developed due to external influences in life). On the other hand different individuals in the species may have variations in their DNA sequences. These genetic variations are the Single Nucleotide Polymorphisms (SNP). This happens on average once for 300 locations, and mostly only one type of exchange is possible, i.e. one *allele*.

Also, if we do not consider any other variation, the Shannon entropy can be calculated from Eq. (3). We assume that the "standard" Human genome sequence is known.

We want to sum up the argument of the Shannon entropy expression, $p_i \ln p_i$, over all base pair configurations. We use the relation for the summation

$$\sum_{i=0}^{2^{N_{bp}}} \to \sum_{i=0}^{N_{bp}} \frac{N_{bp}!}{(N_{bp}-i)!\, i!}.$$

Shannon entropy for a sequence with N_{bp} base pairs and i SNP's is then:

$$H(X) = -\sum_{i=0}^{N_{bp}} \frac{N_{bp}!}{(N_{bp}-i)!\, i!} P_A^i (1-P_A)^{N_{bp}-i} \ln\left[P_A^i (1-P_A)^{N_{bp}-i}\right], \tag{42}$$

where $P_A = 1/300$. This counts up the number of possible SNP changes that may happen.

Notice that [7]:

$$\sum_{i=0}^{N_{bp}} \frac{N_{bp}!}{(N_{bp}-i)!\, i!} P_A^i (1-P_A)^{N_{bp}-i} = 1. \tag{43}$$

The function ln can be rewritten

$$\ln\left[P_A^i (1-P_A)^{N_{bp}-i}\right] = N_{bp}\, \ln[1-P_A] + i\, \ln\left[\frac{P_A}{1-P_A}\right]. \tag{44}$$

Putting this in the above equation we get

$$H(X) = -N_{bp} \ln[1-P_A] - \ln\left[\frac{P_A}{1-P_A}\right] \times \sum_{i=0}^{N_{bp}} \left[\frac{N_{bp}!\, i}{(N_{bp}-i)!\, i!} P_A^i (1-P_A)^{N_{bp}-i}\right]. \tag{45}$$

Since the values of i that contribute the most are around $N_{bp} \times P_A$ we use the approximation that the i in the numerator is a constant instead of a variable.

$$i \to k = N_{bp} P_A \tag{46}$$

We can then approximate $H(x)$

$$H(X) \approx -N_{bp} \ln[1-P_A] - N_{bp} P_A \ln\left[\frac{P_A}{1-P_A}\right] = N_{bp}\left[-P_A \ln\left[\frac{P_A}{1-P_A}\right] - \ln(1-P_A)\right]. \tag{47}$$

We see that $H(X)$ is proportional to N_{bp} and $P_A = 1/300$ so that

$$H_{\max}(X) \approx 0.0223 \cdot N_{bp} = 7.15 \cdot 10^7, \tag{48}$$

for all possible SNP configurations of the Human species. This is much smaller than the entropy corresponding to the maximum possibility of all variations for the DNA of a length of the human genome.

The **spatial configuration of the DNA** can lead to even higher complexity than the base-pair sequence. The spatial area that could be reached by the DNA may reach N_{bp}^3, when the length is N_{bp}. Thus the probability for one configuration could be of the order of N_{bp}^{-2}. On the other hand, our knowledge on the spatial configuration of the DNA of the human genome is little, and the DNA exists in different configurations: curled up in chromosomes, or straightened out at cell division. Thus, to study the entropy arising from the spatial configuration of DNA would require knowledge that we do not have today.

Before cell division, the chromosomes are reshaped and the DNA takes a linearly extended shape (like an extended line), which enables more motion and the replication of the DNA. In this configuration the degrees of freedom in the physical phase space are increased, and thus the entropy of the configuration also increases. This extending of the DNA molecule requires additional energy temporarily. The linear shape allows more motion and increases the possibility of occupying a larger part of the phase space.

Thus the compact curled up configuration of DNA has smaller entropy, having similar amount of freedom as atoms in a solid state, while the linearly extended molecule has considerably larger entropy, similar to a liquid type of structure. So, the entropy of the DNA changes dynamically.

The average **weight of a DNA** can be obtained from its length, $N_{bp} = 3.234 \cdot 10^9$, times the number of atoms per base-pair, 650. Thus $m_{DNA} = 650 \cdot N_{bp}$ AMU $= 3.489 \cdot 10^{-15}$ kg. Consequently in 1 kg we have $N_{DNA} = 2.866 \cdot 10^{14}$ molecules.

Then, from Eq. (40) we get the specific entropy for the DNA base-pair sequence of a single individual. The corresponding entropy in 1 kg of DNA molecules is then

$$S_{1\text{ kg}}^{DNA} = k_B\, N_{DNA}\, \sigma_P^{DNA} = 3.958 \cdot 10^{-1\,947\,000\,000}\ \text{J/K}. \tag{49}$$

9. Entropy of live material tissues

Live material tissues contribute to a high complexity on a larger scale. The best example of this is the nervous system. In a human brain there are about 10^{10} nerve cells, and each of these have about 10^3–10^5 synaptic junctions. This means that the whole nervous system may have up to $N_s = 10^{15}$ synaptic junctions. If we quantize the synaptic couplings as 0 to 1 only, then we have 2^{N_s} different states statically. This can even lead to higher complexity than the DNAs. At the same time it is difficult to estimate, which configurations can be realized, and actually these configurations can change each second. A sleeping persons brain has different entropy than an active one.

To analyse this level of complexity is beyond our present goal.

10. Conclusions

We have demonstrated quantitatively the increasing complexity of materials, and used the entropy for unit amount of material in order to be able to get a measure. This idea stems from Ervin Schrödinger, but our knowledge today makes it possible to extend the level of quantitative discussion to complex live materials.

We may continue these studies to higher levels of material structures, like living species, artificial constructions, symbiotic coexistence of different species, or groupings of the same species. We can even continue up to structures in Human society.

The main achievement of this work is to show how the entropy in the physical phase space and the entropy of structural degrees of freedom (Shannon entropy) can be discussed on the same platform, as shown in Section 3 via Eq. (14). For further developments it is important to point out two fundamental aspects of the entropy concept: (i) the *quantization* of the space of a given degree of freedom, and (ii) the *selection of the realized, realizable or beneficial configurations* from all the possible ones. If we go towards more complex systems, these two questions become non-trivial, and particularly in the case of the utmost complex systems where it is not clear which are the realizable and most beneficial systems. This is already a challenging question in the case of the nervous system, and even more so for organizations in the society or in economy.

The examples presented are all analysed from a static point of view. As we see on the example of the nervous system the dynamical change of the entropy of the system is also important. Furthermore, the speed of development is also important. The early development of complexity happened on a very slow rate, while the development of complexity of the nervous system is many orders of magnitude more rapid then the development of the DNA structure. The dynamics and direction of these changes are also essential, as shown in Ref. [3].

Some specific studies in these directions exist already. See e.g. considerations on general dynamics of sustainable development [9], and on the life-span of different species related to their entropy and metabolism. We are looking forward to further developments [3].

Acknowledgements

Enlightening discussions with Tamás Biró, Stuart Holland, Zoltán Néda, Gábor Palló, István Papp, Péter Ván and Yilong Xie are gratefully acknowledged. This research was partially supported by the Academia Europaea Knowledge Hub Bergen, by the Institute of Advanced Studies, Kőszeg, and by the Research Council of Norway, grant no. 231469.

References

[1] Erwin Schrödinger, What is life? - The Physical Aspect of the Living Cell, The Cambridge University Press, 1944. Based on the Lectures delivered under the auspicies of the Trinity College, Dublin, in February 1943.
[2] Claude E. Shannon, A mathematical theory of communication, Bell Syst. Tech. J. 27 (1948) 379–423;
James V. Stone, Information Theory: A Tutorial Introduction, Sebtel Press, 2015;
Mikhail V. Volkenstein, Entropy and Information, in: Progress in Mathematical Physics, 2009;
Robert M. Gray, Entropy and Information Theory, Sptinger, 2014.
[3] L. Pénzes, L.P. Csernai, Über den Zusammenhang von Lebensdauer, Konstitution und Information, Z. Alternsforschung 35 (1980) 285–296.
[4] L.P. Csernai, I. Papp, S.F. Spinnangr, Yilong Xie, Physical basis of sustainable development, J. Cent. Eur. Green Innov. 4 (2016) 39–50.
[5] L.P. Csernai, Introduction to Relativistic Heavy Ion Collisions, Wiley, 1994.
[6] James F. Lutsko, Marc Bauss, Can the thermodynamic properties of a solid be mapped onto those of a liquid? Phys. Rev. Lett. 64 (1990) 761.
[7] S. Martiniani, K.J. Schrenk, J.D. Stevenson, D.J. Wales, D. Frenkel, Turning intractable counting into sampling: Computing the configurational entropy of three-dimensional jammed packings, Phys. Rev. E 93 (2016) 012906.
[8] Peter Csermely, Kuljeet Singh Sandhu, Eszter Hazai, Zsolt Hoksza, Huba J.M. Kiss, Federico Miozzo, Daniel V. Veres, Francesco Piazza, Ruth Nussinov, Disordered proteins and network disorder in network descriptions of protein structure, dynamics and function: Hypotheses and a comprehensive review, Curr. Protein Pept. Sci. 13 (2012) 19–33.
[9] Tamas S. Biro, Zoltan Neda, Dynamical stationarity as a result of sustained random growth, arXiv:1611.06698 [cond-mat.stat-mech].